



HAL
open science

Demand-side flexibility in a residential district: What are the main sources of uncertainty?

S. Martinez, M. Vellei, Jérôme Le Dréau

► To cite this version:

S. Martinez, M. Vellei, Jérôme Le Dréau. Demand-side flexibility in a residential district: What are the main sources of uncertainty?. Energy and Buildings, 2021, pp.111595. 10.1016/j.enbuild.2021.111595 . hal-03450476

HAL Id: hal-03450476

<https://univ-rochelle.hal.science/hal-03450476v1>

Submitted on 8 Jan 2024

HAL is a multi-disciplinary open access archive for the deposit and dissemination of scientific research documents, whether they are published or not. The documents may come from teaching and research institutions in France or abroad, or from public or private research centers.

L'archive ouverte pluridisciplinaire **HAL**, est destinée au dépôt et à la diffusion de documents scientifiques de niveau recherche, publiés ou non, émanant des établissements d'enseignement et de recherche français ou étrangers, des laboratoires publics ou privés.



Distributed under a Creative Commons Attribution - NonCommercial 4.0 International License

1 Demand-side flexibility in a residential district: what 2 are the main sources of uncertainty?

3 S. Martinez¹, M. Vellei¹, J. Le Dréau¹

4 ¹ LaSIE UMR CNRS 7356, La Rochelle University, France

5 Abstract

6 With the increasing share of intermittent renewable energy sources in the energy mix, demand-
7 side flexibility is likely to play a key role in the future. For buildings, flexibility is defined as
8 the ability to shift their energy consumption away from “peak periods” *i.e.* high-demand periods
9 of the electrical network. In France, these episodes occur mainly during the wintertime due to
10 the significant demand for space heating. To achieve flexibility objectives, we explore an
11 indirect control strategy at district scale by adjusting the dwelling thermostat during peak
12 periods. The study is conducted on 337 dwellings in order to better predict the load curve by
13 taking advantage of the aggregation effect. Three main research questions are addressed in
14 relation to the assessment of flexibility potential: (i) the effect of aggregation, (ii) the
15 identification of the most influencing factors, including occupant behavior, and (iii) the
16 quantification of uncertainties. Using an urban building energy modeling tool populated with
17 various national data sources (building envelope, energy class of equipment, etc), we perform
18 a sensitivity analysis on 22 parameters representing the geometry, the appliances, the building
19 characteristics, the occupants, and the grid. The output indicator is the average power shifted
20 during the flexibility (or demand response) event. From this analysis, 7 parameters appear as
21 being the most influential. A regression analysis on these parameters is performed, depending
22 on both the duration of the event and the typology of the district. The results show that the
23 duration of the flexibility event and the occupant pre-selected temperature change are the most
24 influential parameters. It results to approximately ± 90 W of uncertainty on an average potential
25 of 290 W of shiftable power per household in a recent district. Furthermore, the occupants are
26 highlighted as making a significant contribution to flexibility. Finally, we observed that the
27 thermal properties investigated with the study of an old fabric district play a key role. Low
28 thermal performance means high heating consumption and increased flexibility potential, but a
29 similar relative uncertainty.

30 **Keywords:** urban building energy modeling, bottom-up, district, space heating, demand-
31 response, sensitivity analysis, occupant behavior, probabilistic district characterization

32 1 Introduction

33 1.1 Research background

34 Global warming, fuel poverty, and sustainable development are leading to a growing interest in
35 renewable energy sources, which are often highly intermittent (e.g. solar, wind). As a result,
36 the power grid becomes less robust. In this context, the grid flexibility is defined as the
37 capability of the power system to maintain a balance between generation and load. If the
38 production becomes more intermittent because of an increased share of renewable sources, load
39 adaptation (flexibility) or storage solutions need to be deployed. Consequently, there is an

40 active research field into energy flexibility of the demand. In 2015 Lund *et al.* [1] have
41 published a review of the energy system flexibility measures and point out that the use of
42 dedicated flexibility products such as smart thermostats will become more important with the
43 integration of renewable energies.

44 The building is an interesting lever to increase the flexibility of the grid as it represents about
45 30%-40% of the global energy consumption [2]. Indeed, the electricity share of the world
46 residential energy consumption is expected to reach 43 % by 2040 (39% in 2012). Moreover,
47 by 2025, electricity is expected to overtake natural gas as the leading source of
48 delivered residential energy [3] and space heating is seen as a promising source of flexibility.
49 The main challenge of using the flexibility of residential buildings is the small amount of power
50 involved (a few hundred watts) and their controllability. Indeed, the availability of these flexible
51 loads depends strongly on the preferences and activities of occupants. For an individual
52 building, it is therefore challenging to predict the flexibility potential. At the district level, the
53 diversity of uses allows a more reliable response and an increased thermal storage capacity [4].
54 In addition, for the residential sector, other challenges such as data scarcity and variability in
55 the envelope properties exist.

56 The IEA EBC Annexes 67 and 82 are dedicated to energy flexibility of buildings [5] and
57 document the growing interest in this topic. Several factors have been identified as influencing
58 flexibility in the literature [6], but they are usually evaluated for individual buildings. Putting
59 forward the key role of aggregation, Hu and Xiao [7] recently proposed a quantification of the
60 flexibility at the district scale with a focus on the role of aggregation.

61 1.2 Research gaps

62 When activating energy flexibility in buildings, the aggregation effect has proven to reduce the
63 uncertainty of the predicted power load. As highlighted by Dickert and Schegner [8] for
64 residential applications, electric loads are deeply stochastic. The aggregation effect at the
65 district scale makes the electric load less stochastic than that of a single building, and therefore
66 easier to predict. De Jaeger *et al.* [9] observed a reduction from 65 % down to 10 % uncertainty
67 in the average district energy demand when evaluating a single building compared to 50
68 buildings. The positive effect of aggregation has also been observed experimentally [10]. With
69 more than 20 apartments, the prediction of the space heating needs becomes less stochastic.
70 Therefore, the energy flexibility of buildings becomes interesting at the district scale so that the
71 Transmission System Operator (TSO) can use this potential.

72 To evaluate energy flexibility at district scale, an urban building energy model (UBEM) is
73 required. Different models are available [11–14], most of them being bottom-up physical
74 models. The main differences between these tools are the thermal models used (thermal zoning
75 and discretization) as well as the definition of the input parameters, as pointed out by De Jaeger
76 *et al.* [15]. Indeed, UBEM require the adjustment of many parameters, which can be poorly
77 known and stochastic. These parameters are related to the building properties (geometry,
78 envelope, systems) and to the occupants (activities, user-related equipment). Therefore, the
79 correct characterization of these input parameters and their diversity is a challenge. Probabilistic
80 characterization can be used for this purpose [19]. Moreover, there is lack of validation of these
81 tools, especially in the ability to simulate energy flexibility at small, aggregated level (\approx 100-
82 500 dwellings).

83 To assess the robustness of the results obtained from UBEM, the quantification of uncertainties
84 is necessary. This can be done with a sensitivity analysis (SA). Among the sensitivity analysis

85 techniques, the Morris method has proven its reliability and effectiveness in the building sector.
86 A detailed presentation of the Morris SA method for optical application is given in [16]. In
87 building applications at district scale, De Jaeger *et al.* [9] evaluated the influence of envelope
88 losses on district energy demand. The average nighttime set point temperature was the main
89 occupant-related parameter influencing the district energy demand. For a single residential
90 building, Vivan *et al.* [17] observed that the level of insulation in summer and the time of the
91 demand response (DR) event in winter were the most influential parameters.

92 The accurate estimation of the potential can increase the stakeholders participation in energy
93 flexibility [18]. To correctly estimate the flexibility potential at district scale, it is necessary to
94 identify and quantify the uncertainties arising from both building and occupant parameters. In
95 this context, it is particularly important to model the influence of occupants, as they can greatly
96 alter the flexibility potential. In other words, a sensitivity study highlights the main drivers of
97 flexibility at district scale and can be useful in performing a flexibility audit. However, this has
98 not yet been done to the best of our knowledge, due to the challenging aspects of modelling the
99 stochastic behavior of the occupants.

100 1.3 Research objectives

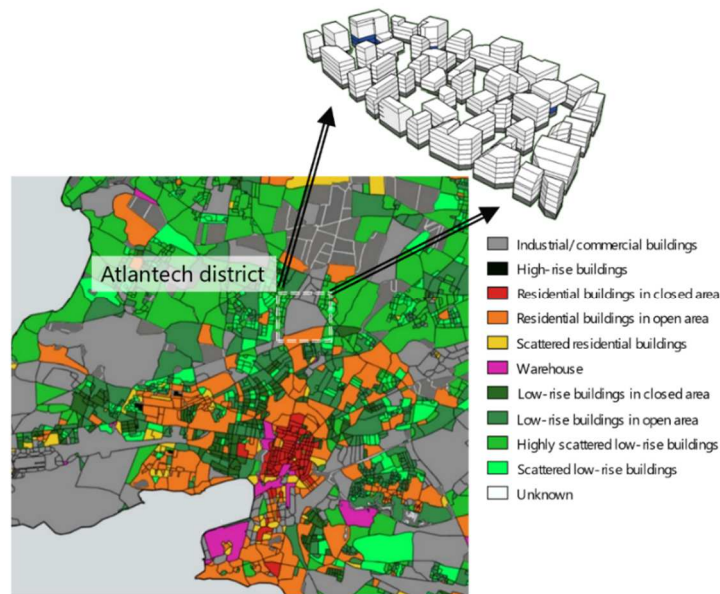
101 This paper proposes a methodology to evaluate the uncertainty on the shiftable heating load
102 when activating a group of buildings using heat pump systems. Facing these challenges, a
103 probabilistic characterization methodology with a district database is proposed in this study.
104 Different set point changes (duration and intensity) will be sent to the dwellings, in which the
105 energy use for space heating will be modulated according to the constraints and flexibility
106 tolerances of the users. The stochastic thermostat adjustment behavior of the occupants will be
107 modelled with an agent-based approach. The influence of the input parameters on the flexibility
108 potential will then be evaluated. The results of this study can be used for different purposes:
109 quantifying the uncertainties for control, listing input parameters for a flexibility audit,
110 evaluating the optimal scale of aggregation, providing guidelines on signal design to increase
111 reliability, etc.

112 To illustrate this methodology, the case study of the Atlantech district (La Rochelle, France) is
113 considered with two levels of building performance (part 2). From this district, an urban
114 building energy model (DIMOSIM) is used to simulate the consumption of buildings (part 3).
115 Finally, a SA using the Morris method and a regression analysis are presented (part 4 and 5).

116 2 Case study

117 2.1 District characteristics

118 The district studied is located in the north of La Rochelle city (latitude 46°2' North, longitude
119 1°1' West, France) in a temperate oceanic climate. The city is mainly composed of low-rise
120 residential multi-storey buildings. The district is composed of 98 buildings divided into 337
121 dwellings. The weather data file corresponds to the year 2017, classified as typical for future
122 weather conditions, which represent 1904 heating degree days (base 21 °C). This district is
123 mainly composed of couples (with or without children). The dwelling floor area varies from 45
124 up to 110 m², with an average size of 65 m².



125

126

Figure 1: Atlantech district case study. Urbanization database comes from [20]

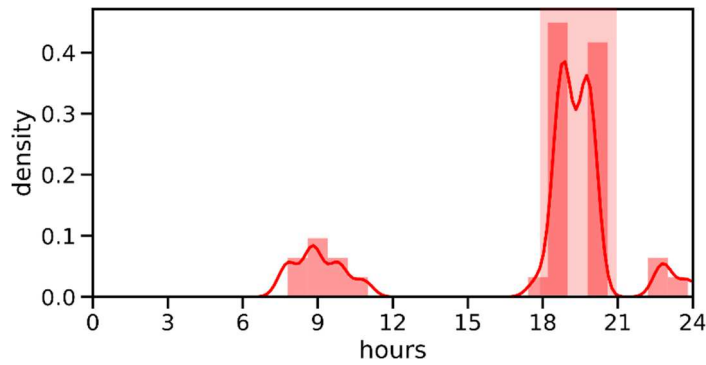
127 Two levels of building performance are considered in this study to assess the influence of the
 128 construction period on energy flexibility:

- 129 ▪ the **new district** (mean consumption for heating of 12 kWh/m².year): the envelope
 130 and system properties are defined in accordance with the current French building
 131 regulation (2012). Space heating is provided by heat pumps and water-based
 132 radiators;
- 133 ▪ the **old fabric district** (mean consumption for heating of 100 kWh/m².year): the
 134 building properties are defined according to the typical characteristics of multi-
 135 storey residential buildings from the period 1982-1989, including renovations.
 136 Space heating is provided by direct electric convectors.

137 In both cases, national databases are used to define the buildings properties (see Annex).

138 2.2 Flexibility signal

139 Flexibility is activated every day over the same period, by an economic incentive such as a
 140 time-of-use tariff. This strategy was selected as it is relatively inexpensive to implement with
 141 smart meters or centralized thermostats. Moreover, it ensures the privacy of the occupants. The
 142 French TSO (2017) provides the peak hour distribution. Peak hours mainly occur in the late
 143 afternoon (Figure 2), when everybody gets back home. Based on this observation, a price signal
 144 is built with a starting time set to 6 pm and a duration from 0.5 up to 3 hours.



145

146

147

Figure 2 : Daily repartition of the 39 peak hours recorded in France for January 2017; the DR event period considered in this study is highlighted in red

148 2.3 Flexibility activation in buildings

149

150

151

152

Once the flexibility signal is sent to the buildings, it needs to be interpreted at the equipment level. To model this flexibility, we based our approach on existing technologies, such as smart thermostats with DR applications [21,22]. The main advantage of this technology is that little extra investment is required, and it ensures the privacy and controllability by users.

153

154

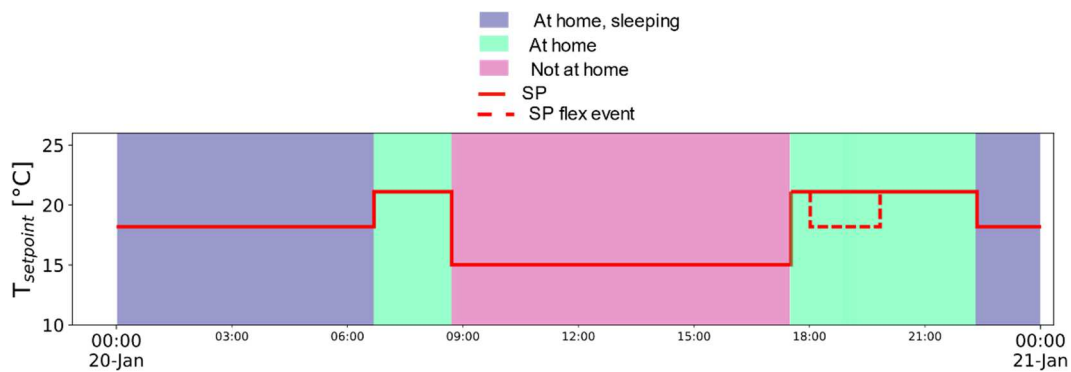
155

156

157

158

The flexibility on space heating is activated semi-automatically by the thermostat of the dwelling, according to the preferences of the occupants (*i.e.* the pre-set tolerated temperature decrease, ΔT). When activated for flexibility, the dwelling set point decreases during the peak period, even if it is unoccupied (Figure 3). In addition, the occupants can interact with the DR signal using the thermostat and modify the set point according to their thermal comfort, which will be discussed in more detail (Section 3.3.2).



159

160

161

Figure 3: Example of temperature set point in a dwelling (comfort set point of 21°C, setback activated at night and for when not at home and tolerance towards flexibility set at -2°C)

162 3 Modeling energy flexibility at district scale

163

164

165

166

167

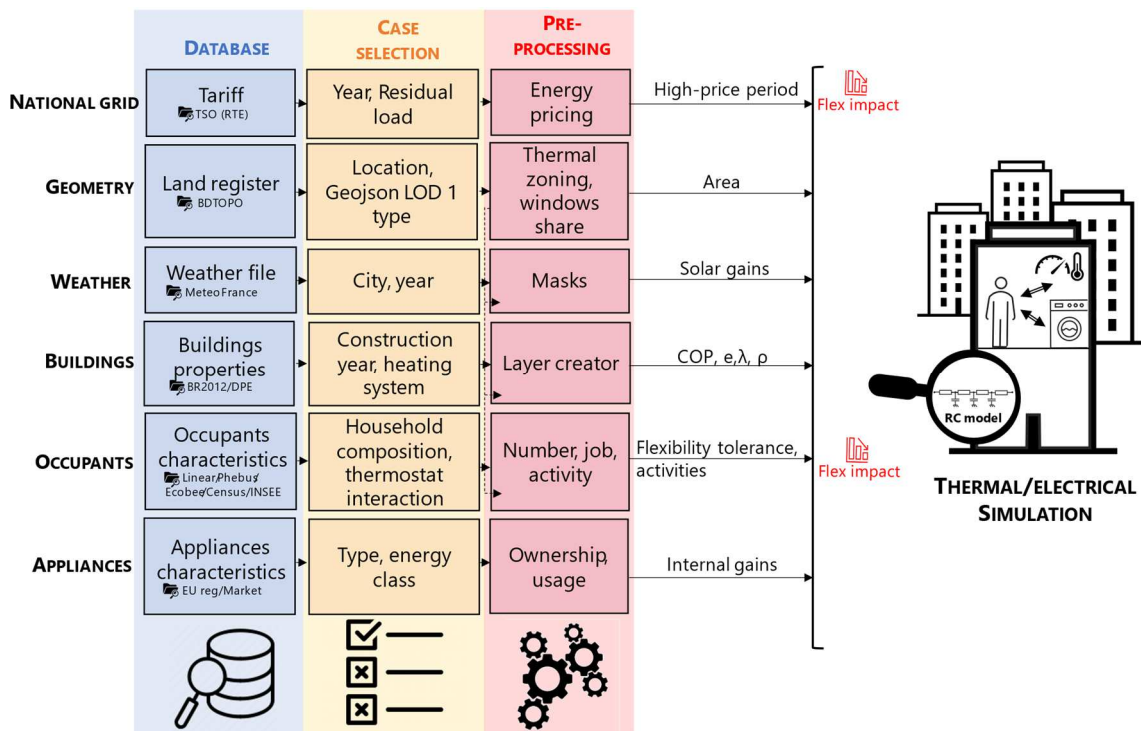
168

The UBEM tool is developed using a bottom-up approach to simulate the thermal and electric load of the residential district. The simulation platform used is a Python-based model (DIMOSIM) developed by CSTB [23–25]. In order to optimize the computation time while affecting the calculation accuracy as little as possible, the recommendations proposed by Frayssinet [26] were followed such as a detailed envelope description to model the heat conduction in walls, a model for the internal mass in order to consider internal inertia of

169 dwellings, a detailed calculation of solar masks to estimate solar gains. The simulation time-
 170 step is set to 10 minutes.

171 Figure 4 provides an overview of the model. The UBEM tools require usually a large amount
 172 of information [27], more than 15 000 inputs were filled in for this study. Among the different
 173 databases listed (in blue on Figure 4) a selection is made according to the case study in order to
 174 obtain a representative dataset. From this selection, preprocessing is performed to convert the
 175 data into usable inputs for building energy models, some of them being represented in Figure
 176 5. When possible, these inputs are added to the UBEM as normal distributions, where the mean
 177 (μ) and standard deviation (σ) are computed from databases (see Annex). In general, normal
 178 distributions appeared as being well representative of the inputs variability observed in the
 179 database. For distributions that do not follow a normal distribution, see for example the number
 180 of occupants in each dwelling in Figure 5b, a random selection of inputs is performed. In Figure
 181 5, the bins represents the discrete sampling of the distributions, while the lines represent the
 182 kernel density estimate of the distribution [28].

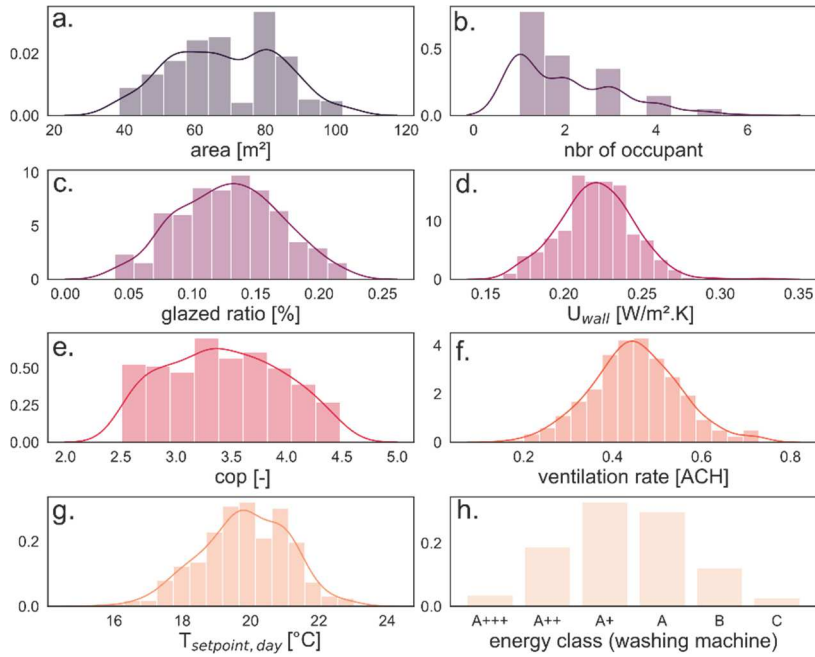
183 The geometry of the district is taken from the land register and the glazing ratio is set according
 184 to the orientation of the dwelling. The weather file is used to compute the solar gains and
 185 represents the boundary conditions for the heat transfer model. The occupant's characteristics,
 186 professional categories, and occupancy rates are given as input to the UBEM. Finally, the usage
 187 habits of the appliances, which influence the electrical load and the internal gains are defined
 188 for each dwelling. A random process generates diversity in the set of input variables.



189

190

Figure 4 : Overview of the modelling process



191

192 Figure 5: Examples of input distributions for the new district model for floor area (a), number of
 193 occupants (b), glazed area ratio (c), wall heat loss coefficient (d), heat pump coefficient of
 194 performance (e), ventilation air change rate (f), set point temperature (g) and energy class of systems
 195 (h)

196 3.1 Geometry

197 The footprint and height of buildings are defined with a land register at LOD1 level of detail.
 198 Then, the buildings are split into dwellings assuming a floor height of three meters. Each
 199 dwelling is modeled as a single thermal zone, which is acceptable due to the small temperature
 200 differences expected between the different rooms [29]. Indeed, the dwellings are characterized
 201 by a small volume, a single set point temperature and an inter-zonal ventilation flow rate. The
 202 geometry of the district is also used to evaluate solar heat gains, taking into account shading
 203 between buildings and openings.

204 3.2 Buildings

205 For each building, the composition of the exterior and interior walls, the windows, the floor,
 206 and the roof is defined according to the current building regulation [30] or the energy audit
 207 database [31]. The databases are analyzed in order to obtain a mean value (μ) and a standard
 208 deviation (σ) for the distribution of each parameter.

209 Space heating is provided by air/water heat pumps for the new district and by electric convectors
 210 for the old fabric district. Air-to-water heat pumps are variable speed. The coefficient of
 211 performance (COP) of the heat pumps is based on a polynomial regression from the nominal
 212 COP to estimate the thermal power output as a function of the temperature difference between
 213 the sink (*i.e.* the building) and the source (*i.e.* ambient air temperature). Such a technique,
 214 illustrated in [32], has been adapted in the model. The sizing of the heating systems is carried
 215 out with an oversizing coefficient of 20 % and the supply water temperature is set to 45°C for
 216 the heat pump systems.

217 Ventilation and infiltration are set according to measurements performed in French households
218 [33]. It is assumed that the dwellings are equipped with mechanical ventilation, humidity-
219 controlled in the case of the new district and constant for the old fabric district. Infiltration is
220 modeled as a constant airflow system, based on n_{50} measurements.

221 3.3 Occupants

222 This section describes the main elements of the occupant model: household composition and
223 professional category (3.3.1), occupant activity and presence (3.3.2) and household set point
224 schedule (3.3.3). These models have been introduced, validated, and used in our previous works
225 [34–36].

226 3.3.1 Household composition and professional category

227 We first assign a composition to each dwelling by sampling with replacement from the
228 conditional distribution of the household composition conditioned on the usable floor area of
229 the dwelling. These conditional distributions are derived using the summary tables from the
230 INSEE 2015 population census data [37]. The original INSEE household composition
231 categories are simplified using 11 main categories (single adult living alone, single adult with
232 (1,2,3,4) children, couple without children, couple with (1,2,3,4) children, other type).

233 The professional category (employed, unemployed, student or retired) based on the household
234 reference person is assigned by sampling with replacement from the conditional distribution of
235 the professional category conditioned on the household composition. The status of any other
236 member of the household is assigned based on additional summary tables dedicated to families.
237 Children are assumed to be students.

238 3.3.2 Occupant activity and presence

239 To model occupants' activity and presence, we retain the activity sequences or activity profiles
240 available from the French Time Use Survey (TUS) data (2009-2010 TUS campaign) [38].
241 About 27,900 daily logbooks are used to build the model. These daily times series are clustered
242 according to the professional category of occupants (employee, retired, student, etc) and the
243 type of day (weekend vs. weekday). These two parameters have been selected out of eight
244 independent descriptors as they were identified as influencing the most the activities of
245 occupants [34]. Based on the assumption that most human behaviors are characterized by daily
246 routines, a hierarchical agglomerate clustering is performed within each group to find clusters
247 of similar daily profiles. This clustering used the Jaccard distance as metric and Ward's linkage
248 criterion to group similar schedules, while the number of clusters was identified through the
249 elbow method.

250 To implement the occupants' activity time series in the UBEM, a stochastic procedure is applied
251 to create different yearly activity patterns by randomly drawing daily schedules within the
252 cluster corresponding to the professional category of occupant and type of day simulated. The
253 outputs of this model are the activities and presence for each occupant of the household.
254 Compared to probabilistic approaches, this method directly uses actual TUS activity sequences
255 and, therefore, allows accounting for the diversity of the real population in terms of occupancy
256 and domestic activities [39].

257 The activity time series are then converted into time series of metabolic heat rate by using
258 distributions obtained from the ASHRAE reference tables of metabolic rates for common
259 activities [40]. The estimated metabolic heat associated with the occupant's activity is, in turn,

260 an input of the dynamic thermal comfort model. While the status of the occupant (at home, at
261 home sleeping, not at home) is an input of the thermostat adjustment model.

262 3.3.3 Set point schedule

263 In our occupant modeling approach, we assume that each household is equipped with a
264 programmable thermostat (see Section 2.3), which can be used to set a schedule for:

- 265 ▪ $T_{\text{setpoint, day}}$: the day set point temperature when somebody who is not sleeping is at home;
- 266 ▪ $T_{\text{setpoint, night}}$: the night set point temperature when everybody who is at home is sleeping;
- 267 ▪ T_{setback} : the setback temperature when nobody is at home.

268 For each household, the schedule is estimated based on the occupants' activity and presence
269 profile time series by calculating the hourly probability of having each household's status (at
270 home, at home sleeping, not at home) over the simulated period. For each hour of the day and
271 depending on the activity of the occupant, the status with the highest probability of occurring
272 defines the corresponding hourly scheduled/default temperature for the household. This hourly
273 profile is repeated for each day (Figure 3). Thus, the hourly set point schedule is defined for
274 each household in a pre-process with respect to the dynamic thermal simulation, while the
275 manual thermostat adjustment behavior is dynamically simulated.

276 Defining an operation schedule does not necessarily imply that each household is using a night
277 set point temperature or a setback temperature. The probability of using either a night set point
278 temperature or a setback temperature is equal to 80 % based on the PHEBUS dataset [41]. The
279 $T_{\text{setpoint, day}}$ distribution is also based on the PHEBUS dataset (Figure 5). Each occupant adapts
280 its default clothing level based on the $T_{\text{setpoint, day}}$ in order to obtain a neutral PMV value. The
281 default clothing insulation and the default set point temperature can then be modified by the
282 occupants over the course of the dynamic simulation (see 3.5).

283 3.4 Appliances

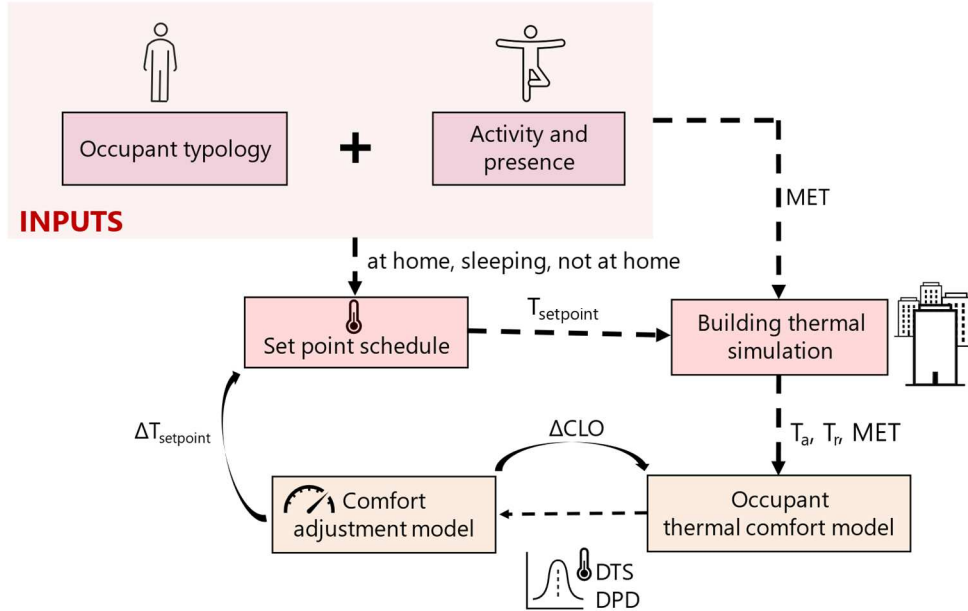
284 The appliances are randomly allocated to the households based on the appliances' ownership
285 rate conditioned on the household size and the professional category and calculated using
286 aggregated data from the PHEBUS dataset [41]. As the conditional distributions were not
287 available, the capacity and energy class of the appliances cannot be conditioned on the
288 household size and the professional category. The marginal distributions of the capacity of the
289 appliances were available from the ADEME survey campaign [44]. The marginal distributions
290 of the energy class of the appliances were built from the marginal distributions of the age of the
291 appliances combined with sales data [49].

292 The appliances' electricity load curves are randomly assigned to the activity starting times
293 based on the capacity and the selected energy class of the equipment (ranging from A+++ to
294 C). In total, 1200 load curves are built based on the EU labeling scheme for electronic devices.
295 The electrical load is then converted into internal heat gains according to emission factors. In
296 total, approximately 85 % of the electricity used by appliances is converted into internal heat
297 gains, which is in accordance with [42].

298 3.5 Modeling flexibility from occupants

299 Occupant thermostat adjustments can occur because of rejection of DR events, change of
300 metabolic rate, or thermal discomfort due to mismatch between schedule and presence (Figure

301 6). The thermostat adjustment behavior is modeled using an agent-based approach: each
 302 member of the household is represented as an agent with a set of attributes (status, clothing, and
 303 metabolic rate) and a set of possible adaptive actions (set point and clothing adjustment). User
 304 interaction data from about 9,000 connected Canadian thermostats included in the Donate Your
 305 Data (DYD) dataset [43] are used to calibrate the thermostat adjustments model [21].



306
 307

Figure 6 : Overview of the modelling framework for thermostat interactions.

308 The adaptive principle [44] is assumed to be determining the manual overriding behavior. For
 309 modeling the agent's adaptive behavior, we use a particular type of agent: the Belief-Desire-
 310 Intention (BDI) agent [45]. In this study, environmental and personal conditions form the
 311 agent's thermal dissatisfaction, which is represented by the Dynamic Thermal Sensation (DTS)
 312 and Dynamic Percentage of Dissatisfied (DPD). DTS and DPD predictions are based on a
 313 thermo-physiological model coupled with a dynamic thermal perception model [35]. This
 314 dynamic evaluation of thermal comfort appears necessary given the short timescale associated
 315 with demand response events.

316 Then, the agent translates its thermal dissatisfaction into a desire about what to achieve. This
 317 action is predicted using a time-dependent Bernoulli process. A uniformly distributed random
 318 number (n) in $[0,1[$ is compared to the DPD. If the DPD is higher than n , the outcome is to
 319 change its current state. The agent's intention is defined by the probabilities of adjusting during
 320 a 2-min time interval (using a time-dependent Bernoulli process):

- 321 1- the clothing $p_{adj, clothing}$ (before), with a mean value of 10.5 % and an observed range of
 322 3-18% based on the calibration with the DYD dataset,
- 323 2- the set point temperature $p_{adj, SP}$ (afterward), with a mean value of 3.5 % and an observed
 324 range of 1-6%.

325 Thus, it is assumed that the adjustment of the clothing insulation is the preferred adaptation
 326 strategy.

327 When the agent decides to adjust its clothing, he does it by either increasing or decreasing the
 328 clothing of $\Delta CLO = 0.1$ clo where 0.1 clo is, for example, the clothing insulation change made

329 when passing from a thin long-sleeved sweater to a thick long-sleeved sweater [46]. While,
330 when the occupant decides to adjust the set point of $\Delta T_{\text{setpoint}}$, he does it to restore thermal
331 neutrality (*i.e.* towards a PMV ~ 0). The $T_{\text{setpoint}+\Delta T_{\text{setpoint}}}$ has a lower limit equal to $T_{\text{setpoint,day}}$
332 -1°C during warm exposures and an upper limit equal to $T_{\text{setpoint,day}}+6^{\circ}\text{C}$ during cold exposures,
333 based on observations of the DYD dataset.

334 3.6 Thermal/electrical models

335 The building thermal model is a detailed physic-based RC model [23]. The elements of the
336 dwelling are discretized into exterior walls, windows (divided per orientation), interior walls,
337 floor, and roof. The opaque walls are discretized in four layers, namely the external finish, the
338 thermal mass, the insulation, and the interior finish, which leads to more than 20 capacities for
339 each thermal zone. The conduction through the walls is then solved by the finite difference
340 method, with a time-step of 10 minutes.

341 The electrical load of the buildings is calculated from the space heating and the equipment
342 consumption on a 10-minute time-step.

343 3.7 Qualitative validation of the model

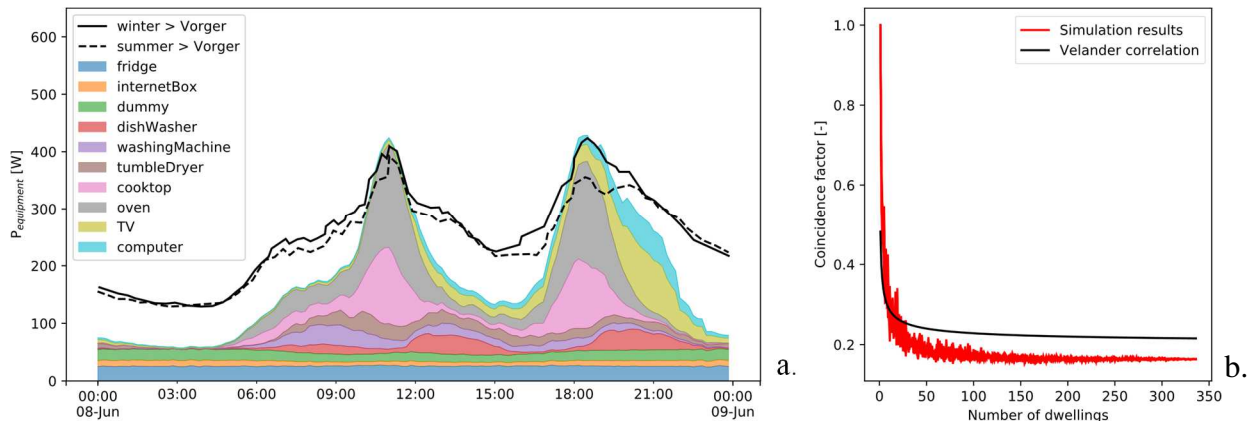
344 Validating the results of UBEM tools is a challenging task due to the lack of standardized data,
345 the lack of information and the complexity of the tools. Comparison with measured data cannot
346 be performed because only half of the Atlantech district has been built to date. Therefore, the
347 model validation focused on the thermal model, the input parameters, and the simulation results
348 with external references.

349 The thermal model of the DIMOSIM tool was compared with the results of the benchmark tests
350 BESTEST [47] (free-running and heating cases) and DESTEST [48]. DIMOSIM shows good
351 agreement with the other tools, both in terms of temperature and energy.

352 Given the large number of input parameters required for the design of the district (around
353 15 000 for this district), the control of these parameters with typical values is of main
354 importance. The heat loss coefficient (HLC) of each dwelling was compared to ensure the
355 overall performance of the district. Additionally, each energy usage was also checked.

356 Figure 7a represents the average daily electrical load profiles of the devices within the district.
357 The average daily profile was compared with the results of Vorger [49]. Vorger's results, also
358 based on a bottom-up model, correspond to the mean power of 100 dwellings randomly
359 selected. The differences observed can be partly explained by the better energy classes selected
360 for the electrical appliances, especially for the fridge. Moreover, Vorger's results are focused
361 on a French representative set of buildings that includes single-family houses equipped with
362 more electrical devices than dwellings. The simulated annual electricity consumption of the
363 appliances ($27 \text{ kWh/m}^2_{\text{heated area}} \cdot \text{year}$) corresponds to the mean value measured in French
364 collective buildings [42]. Additionally, the coincidence factor was assessed to verify the
365 diversity of uses within the district (Figure 7b). This factor is equal to the peak load of a district
366 divided by the sum of the peak loads of its individual buildings. These values are compared to
367 the relationship proposed by Velander (1947) for the energy consumption of appliances with
368 electrical heating. The diversity of uses appears to be consistent within the district, slightly
369 below the values proposed by Velander. Similar observations were made by Sørensen *et al.*
370 [50], in which the measured peak power was about 20% lower than Velander's formula (for
371 1000 apartments). The resulting heating consumption of the new district is equal to 12

372 kWh/m²_{heated area}·year with a relatively large standard deviation between dwellings. Despite
 373 similar thermal properties, not all buildings can benefit from passive solar heat gains within the
 374 district.

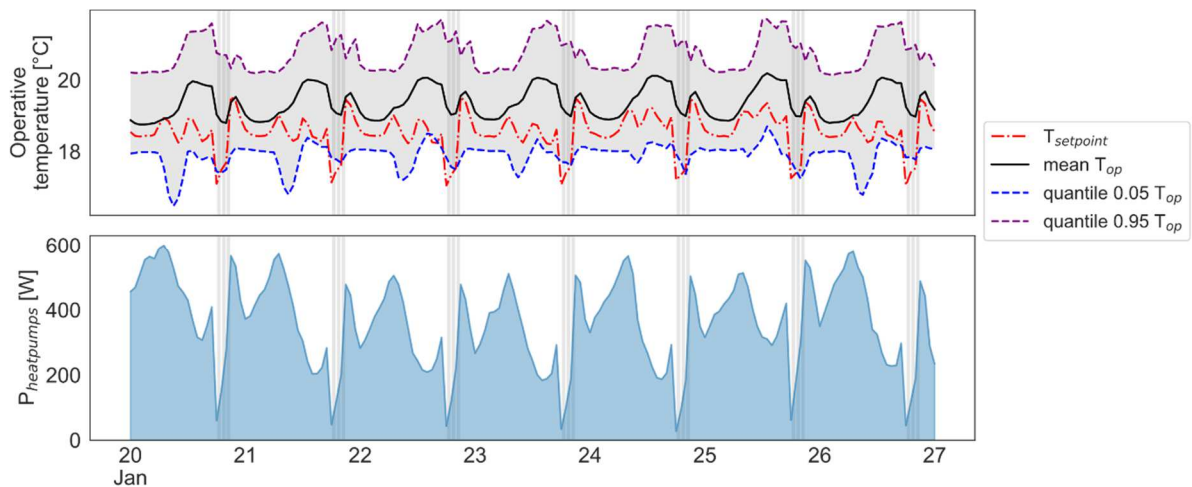


375
 376 Figure 7: Average electrical load per household from appliances, heating excluded (a)
 377 and coincidence factor, heating included (b).

378 3.8 Examples of load curves

379 The time series representation of the UBEM output is presented (Figure 8) for the district and
 380 for three cold days of the winter (20th to 23rd of January). The DR event occurs between 6 and
 381 9 PM, during which the set point is lowered in each dwelling with a different amplitude. The
 382 results presented are the average values of operative temperature and heat-pump electrical load
 383 for the district. The upper graph presents the average set point, the 0.95 and 0.05 quantile of the
 384 operative temperature distribution and the average operative temperature of the dwellings,
 385 while the lower graph represents the average electrical load of the heat pumps.

386 During the day, there is a significant gap (about 2 °C) between the average operating
 387 temperature and the set point. This can be explained by the fact that the set point is reduced
 388 during unoccupied periods (15 °C of set point when dwellings are unoccupied), while inertia
 389 and solar gains have the effect of maintaining the operative temperature. During the flexibility
 390 event, the thermal inertia of the housing explains the gap between the set point temperature and
 391 the operative temperature.



392
 393 Figure 8: Overview of the time series collected as the output of the UBEM during 3 days of January

394 4 Methods

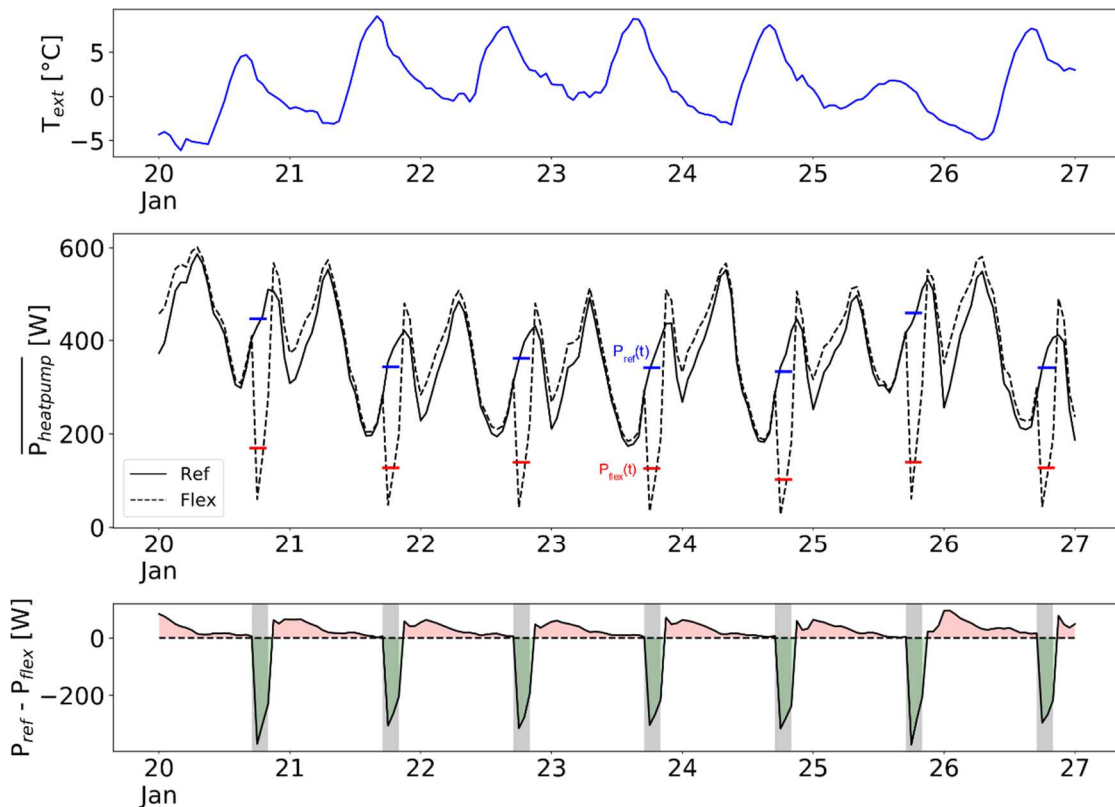
395 4.1 Indicator to characterize flexibility

396 The most common indicators found in the literature to characterize the flexibility are the amount
 397 of power change, duration of the change, rate of change, response time, shifted load and
 398 maximal hours of load advance [1,51,52]. Based on the previous works, we have decided to
 399 consider the mean power shifted away from a peak period to assess flexibility at the district
 400 scale. Since most peak hours occurs during the winter, we decided to focus on January, which
 401 was the coldest month of the year 2017. The average shifted power during a peak period is
 402 given by:

$$P_{\text{shifted}} = \sum_{\text{peak hours}} \sum_{\text{dw}} \frac{P_{\text{ref,dw}}(t) - P_{\text{flex,dw}}(t)}{N_{\text{dw}} \cdot N_{\text{peak hours}}} \quad (2)$$

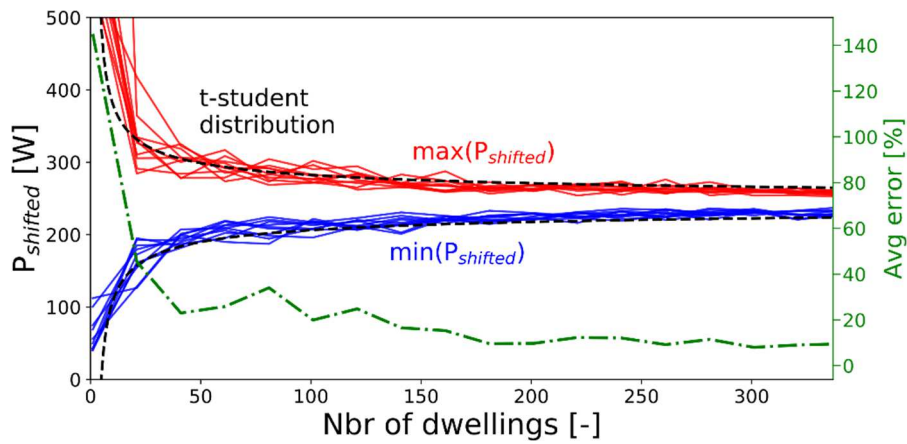
403 Where $P_{\text{ref,dw}}$ is the heat pump electric load (in W) during peak hours for the reference case, i.e.
 404 without DR event, $P_{\text{flex,dw}}$ the heat pump electric load (in W) during the DR event, $N_{\text{peak, hours}}$
 405 the number of peak hours during January and N_{dw} the number of dwellings (dw).

406 To illustrate the calculation of the indicator, we show the evolution of the district-averaged heat
 407 pumps power for both reference and flexibility cases (Figure 9). The simulation focuses on the
 408 average electrical power of air-to-water heat pumps in the 337 dwellings of the district. The
 409 long-lasting rebound effect can be observed. It is useful to recall that, in our model, the
 410 occupants adjust the set point temperature during peak hours in case of thermal discomfort.



411
 412 Figure 9 : Example of a response of the mean electrical power of the heat pumps, new district case-
 413 study

414 The aggregation effect on the electrical load prediction is highlighted in Figure 10. The
 415 indicator was calculated from 1 to 674 dwellings to evaluate the effect of the district diversity
 416 (both from buildings and occupants). From Figure 10, we observe that the increase in the
 417 number of dwellings reduces the uncertainty in the calculation of the indicator. In green, the
 418 average error, defined as the ratio of distance between the maximum and the minimum value of
 419 P_{shifted} to the mean P_{shifted} value, is represented. 337 dwellings appear sufficient to obtain a robust
 420 calculation (10% error). The uncertainty in the value of P_{shifted} , depending on the number of
 421 dwellings, follows a Student's t-distribution with a 95 % confidence interval that is
 422 representative of a random behavior in the sample. According to the t-student distribution
 423 results, a district of 500 dwellings is needed to estimate the P_{shifted} indicator with an error of 5%.
 424 Wang et al. [53] found that 700 dwellings were necessary to decrease uncertainty under 10 %.
 425 These differences can be explained by several facts: (i) in Wang's study the shiftable power is
 426 not averaged over the entire DR event and (ii) the flexibility is only activated during unoccupied
 427 hours leading to a reduced number of considered households, (iii) in our study the period of
 428 activation of flexibility starts at 6 PM, which is a time when the probability of dwellings being
 429 unoccupied is low.



430
 431 Figure 10: Aggregation effect on the mean shifted power calculation, minimum (blue), maximum (red)
 432 values and average error (green)

433 4.2 Identification of the most influential parameters: the Morris method

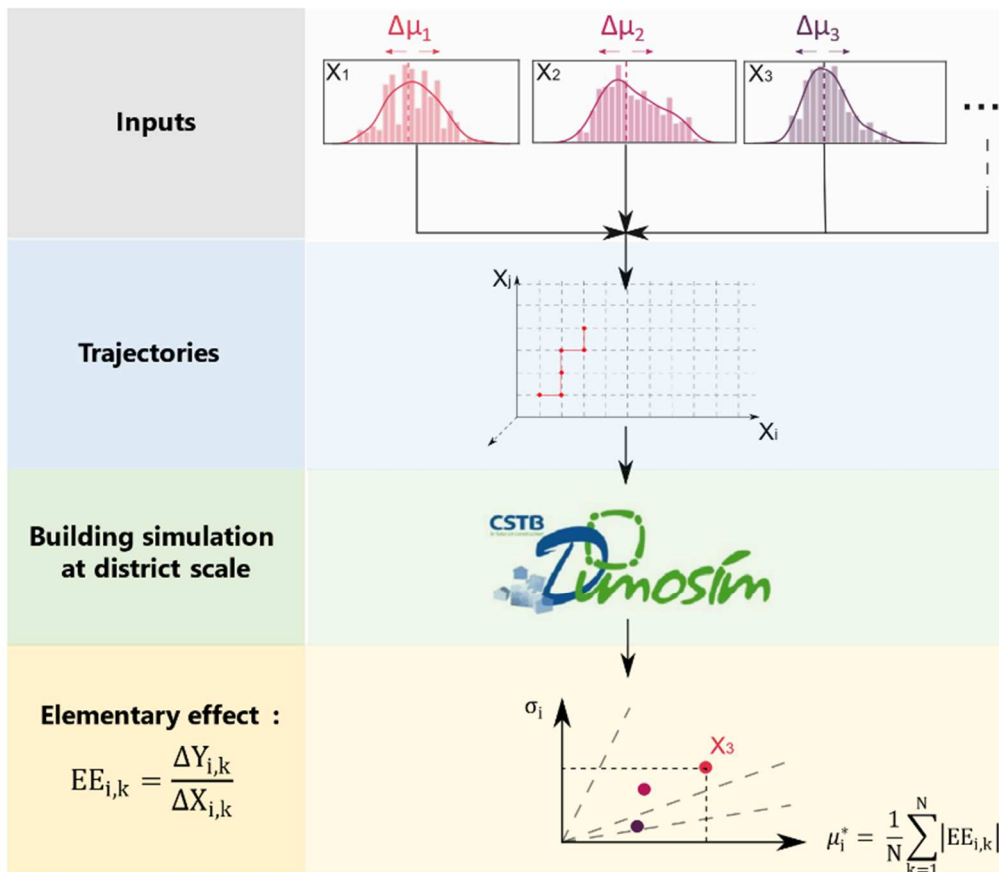
434 The method of Morris [54] consists of segmenting the model inputs within their range of
 435 variation. Thus, this segmentation generates a unit hypercube of input variables that will be
 436 used in the model to evaluate the change in the output for each parameter variation. The
 437 sensitivity measured at each point (elementary effect) can be defined by the ratio between the
 438 output and the input displacement. For a user-defined number of trajectories, the Morris method
 439 evaluates the mean and the standard deviation of the elementary effect. For this study, the input
 440 parameters are assumed to have a uniform distribution. For the 22 selected parameters
 441 concerning buildings characteristics, occupant and appliances, the mean values (μ) of the
 442 distribution are changed and their impacts on the flexibility potential is assessed. The output
 443 considered is the flexibility potential (see 4.1).

444 This screening method has been widely used and described in the literature [55–57] including
 445 for building applications [58]. The method of Morris method appears as a robust and time-
 446 efficient method. For these reasons, it was selected for this study.

447 To process a Morris sensitivity analysis, it is necessary to:

- 448 ▪ define a set of relevant parameters;
- 449 ▪ determine their range of variation;
- 450 ▪ select an indicator that is well suited to the phenomenon under study.

451 The originality of this sensitivity analysis comes from the fact that the inputs are not
 452 deterministic values but normal distributions. Figure 11 provides an overview of the method
 453 used.



454
 455 Figure 11 : Overview of the methodology, from input definition to analysis of the results

456 In Figure 11, EE represents the elementary effect, $\Delta Y_{i,k}$ is the output difference for the k
 457 parameter at the i -th trajectory defined as $f(X_i + \Delta x) - f(X_i)$ where f represents the UBE
 458 $\Delta X_{i,k}$ is the grid step of parameter k , for the i -th trajectory.

459 To determine the most influential parameters, we conducted a 100-trajectories and 4-grid jump
 460 test with the parameters listed in Table 1. The grid jump is the number of samples into which
 461 each parameter is divided. The convergence of the results was checked and found to be well
 462 suited for the identification of the influential input parameters.

463 In Table 1, the parameters (i) are well defined and the determination of (μ, σ) was done by
 464 database analysis (part 3 and Annex 1). The mean of the input is changed between $\mu - \Delta\mu$ and
 465 $\mu + \Delta\mu$ based on the standard error of the mean ($\Delta\mu = 2 \times \sigma / \sqrt{n}$, with $n=98$ buildings). Diversity in
 466 the district will be provided by the standard deviation (σ) of the distribution, which remains
 467 unchanged. The parameters (ii) are derived from a limited set of data, therefore, for these

468 parameters we have defined a 10 % uncertainty on the mean, or an ad hoc value of this
 469 uncertainty. The parameters (iii) are set equally for all the dwellings of the district.

470 In addition to the parameters presented in Table 1, the influence of the building and occupants’
 471 diversity and stochasticity was evaluated. In the UBEM tool, these random processes are
 472 characterized by two parameters:

- 473 1. the random characteristics parameter ($\text{random}_{\text{characteristics}}$), which influences the selection
 474 of occupant and building properties. It allows the district to be populated with a diversity
 475 of occupant and building characteristics;
- 476 2. the random occupant behavior ($\text{random}_{\text{occupant}}$), which influences the sequencing of the
 477 occupant behavior model (presence, activities and thermostat adjustments). It allows to
 478 simulate the stochasticity of occupant behavior.

479 Table 1 : Parameters of the sensitivity analysis, mean value, standard deviation, and range of
 480 variation (“-“ means that no variation among buildings was defined)

	Name	Description	μ	σ	SA bounds [$\mu-\Delta\mu$; $\mu+\Delta\mu$]	unit	
Geometry	glazedRatio	Average glazed ratio of the dwelling	13.5	3	[13, 14]	%	
Buildings	Uwall	Heat loss coefficient of the walls	0.22	0.035	[0.21, 0.23]	W/(m ² K)	(i)
	Uwindow	Heat loss coefficient of the windows	1.23	0.16	[1.2, 1.26]	W/(m ² K)	
	Ufloor	Heat loss coefficient of the floor	0.2	0.055	[0.19, 0.21]	W/(m ² K)	
	Uroof	Heat loss coefficient of the roof	0.13	0.042	[0.12, 0.14]	W/(m ² K)	
	Q _{ventil}	Air change rate (ventilation & infiltration)	0.55	0.15	[0.49, 0.61]	vol/h	
	massthickness (iii)	Equivalent thickness of the concrete core to model the inner mass	0.1	-	[0.05, 0.15]	m	
	COP	COP of the air/water heat pump	3.33	0.81	[3.17, 3.49]	-	
Appliances	cooktop	Energy class of the cooktop	5.1	0.8	[4.94, 5.26]	-	(ii)
	tumbledryer	Energy class of the tumble dryer	5.15	0.72	[4.98, 5.28]	-	
	dishwasher	Energy class of the dishwasher	3.12	1.13	[2.9, 3.36]	-	
	fridge	Energy class of the fridge	3.52	0.94	[3.33, 3.71]	-	
	oven	Energy class of the oven	5.11	0.8	[4.99, 5.31]	-	
	washingmachine	Energy class of the washing machine	2.75	1.24	[2.51, 2.99]	-	
Occupant	setpoint	Average heating set point (day) of the building	19.83	1.26	[19.58, 20.08]	°C	(iii)
	setback	Probability of a dwelling to decrease its set point when unoccupied and sleeping	80	10	[72, 88]	%	
	ΔT	Pre-set set point difference during a flexible event	1.5	0.5	[1, 2]	°C	
	padjSP	Probability for occupant to adjust their set point due to discomfort	3,5	-	[1, 6]	%	
	padjclothing	Probability for occupant to adjust their clothing due to discomfort	10,5	-	[3, 18]	%	
	presence	Probability of occupancy of the dwellings	100	-	[80, 100]	%	
Grid	durationEvent	Duration of the flexibility event	105	-	[30, 180]	min	(iii)

481

482 4.3 A better understanding of the uncertainty of parameters: the regression 483 analysis

484 For the most influential parameters identified by the SA, another computation is made by
 485 modifying “step by step” the parameter, holding other factors constant, and performing a linear
 486 regression analysis of the flexibility potential indicator (P_{shifted}). The impact of the parameter is
 487 quantified using the following three indicators:

- 488 ▪ The **mean value** of the P_{shifted} , represents the average value of the flexibility potential for
489 each parameter tested;
- 490 ▪ The **range of variation** (Δ) between the maximum and minimum value of the flexibility
491 potential (P_{shifted}) gives an idea of the variability of the parameter;
- 492 ▪ The **R^2 coefficient** calculation indicates the predictability of the impact of this parameter
493 on the flexibility potential of the district.

494 **5 Results**

495 We first identify the parameters influencing the most the flexibility of the new district (part
496 5.1). We will later study the performances of a typical old fabric district (part 5.2).

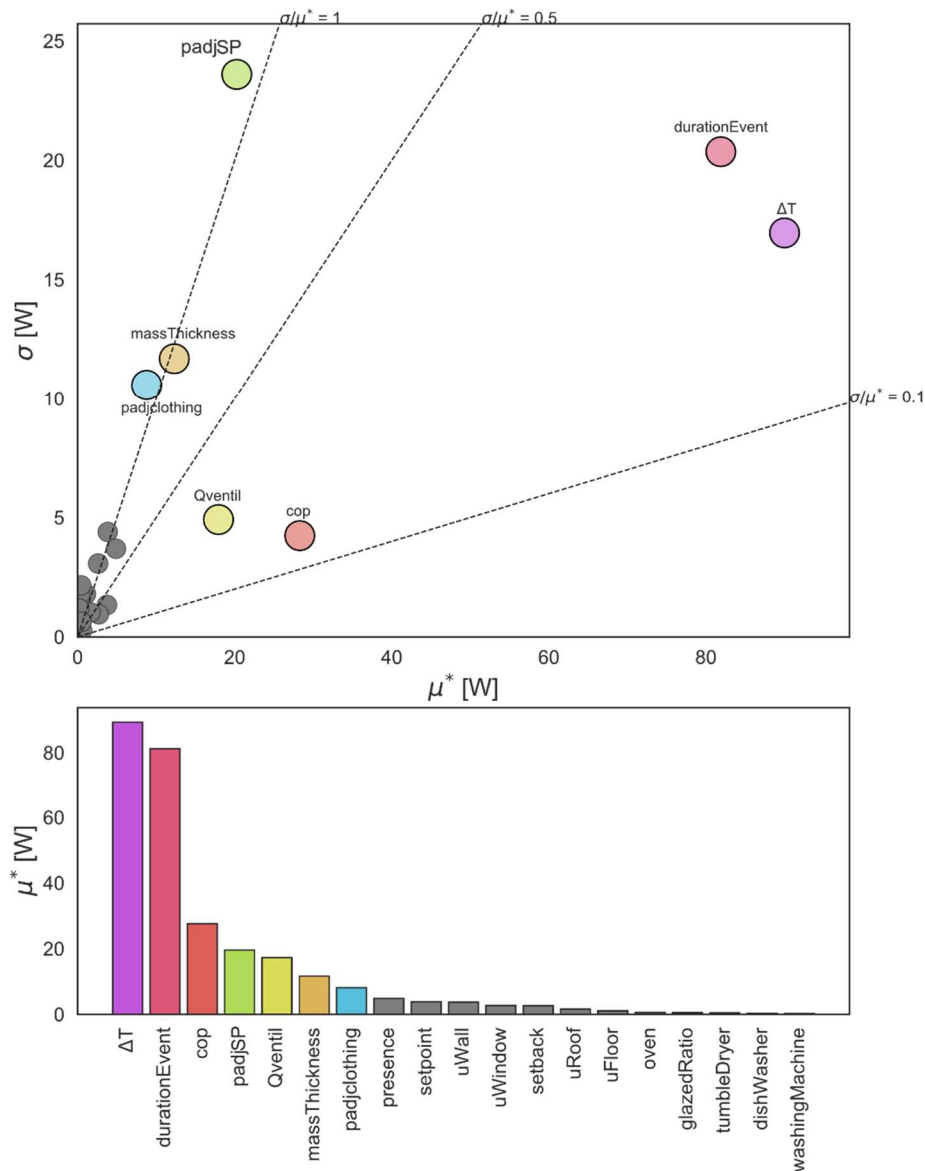
497 5.1 New district

498 5.1.1 Morris screening method

499 Figure 12 presents the results of the sensitivity analysis for the new typical district. The Figures
500 represent the SA-mapping of the parameter and the μ^* distribution. Most of the investigated
501 parameters are considered as little dependent on each other because they are below $\sigma/\mu^* = 1$
502 [54]. Moreover, the limited number of trajectories explain some high values (*i.e.* in the order of
503 magnitude of the mean effect) of the standard deviation of the parameters. However, we
504 consider these results robust enough in order to detect the most influential parameters.

505 With regard to the random parameters, it appears that a Morris sensitivity analysis is not suitable
506 to explore their influence. Thus, we decided to explore these elements separately in Section
507 5.1.2.

508

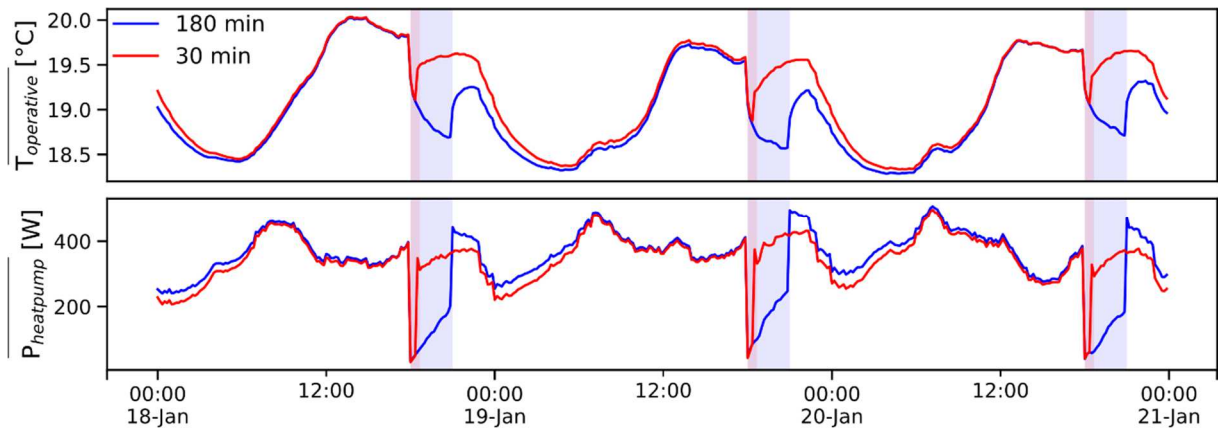


509

510 Figure 12: Sensitivity analysis, σ - μ^* plot and μ^* distribution for the average shifted electrical power
 511 of the district during the month of January – $P_{shifted\ avg} = 290\ W$

512 The average flexibility potential ($P_{shifted}$) was calculated at 290 W. It appears that the duration
 513 event (*durationEvent*) and the set point decrease during the flex event (ΔT) are the key
 514 parameters of the study as its μ^* value (80 W) represents approximately 30 % of the average
 515 flexibility potential. Therefore, these two parameters need to be known by the
 516 aggregator/district manager to evaluate correctly the flexibility potential.

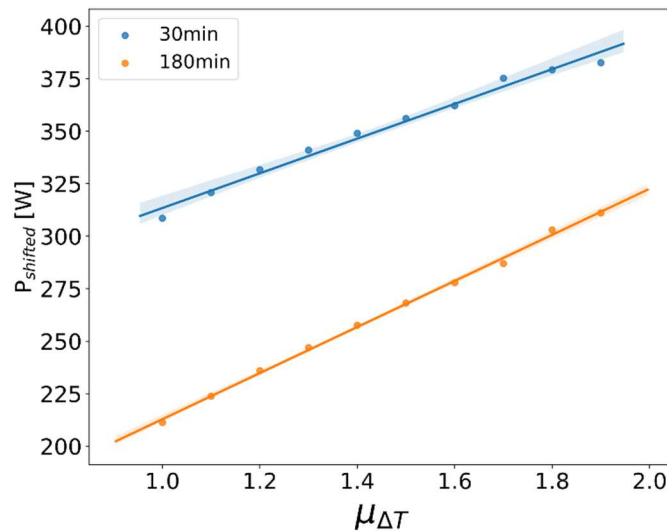
517 An illustration of the importance of the duration of the event on the flexibility potential is
 518 presented below. On Figure 13, the increase in the electrical load after the shutdown of the heat
 519 pumps (especially for the long modulation) indicates that some households have reached their
 520 lower set point. Moreover, the longer the flexibility event, the more likely the operative
 521 temperature in the dwelling will decrease below a comfort temperature, so an adjustment in the
 522 set point from occupant will occur to increase the indoor temperature.



523
524
525

Figure 13 : Effect of the event duration on the average operative temperature and the average heat pump consumption

526 Thus, we observe that the event duration indicator can modify the influence of other parameters.
527 Figure 14 shows the combined effect of $durationEvent$ and ΔT . For a short modulation, we
528 detect that $P_{shifted}$ is higher compared to a long modulation as the operative temperature is less
529 likely to reach the lower set point due to thermal inertia. Thus, no matter how low the set point
530 temperature is, the heating system will stop. Consequently, the flexibility potential will be less
531 dependent on the temperature difference (lower slope of the regression line).



532

533 Figure 14 : Influence of the set point decrease and duration of the DR event on the flexibility potential.

534 The third most influential parameter is the efficiency of the electrical to heat conversion of the
535 heatpump system (cop , $\mu^* = 30$ W). Then, the probability of thermostat adjustment ($padj_{SP}$) is
536 observed to be influential ($\mu^* = 20$ W). The ventilation rate (Q_{ventil}) plays also an important
537 role in the flexibility potential evaluation as it represents a non-negligible part of the thermal
538 losses in these well-insulated buildings. For similar reasons, the $massThickness$ influences the
539 $P_{shifted}$ value as it represents the thermal inertia of the housing partitions. Finally, the probability
540 of clothing adjustment ($padj_{clothing}$) is observed as being important. This parameter, and also
541 $padj_{SP}$, are related to the behavior of the occupants. An increase in the probability of thermostat
542 adjustment leads to an increase in the probability of rejection of the flexibility event, and thus
543 a decrease in the flexibility potential of the neighborhood. Conversely, an increase in the

544 likelihood of thermal comfort adjustment through clothing changes will decrease the number
545 of rejections, and thus increase the flexibility potential. The 7 coloured parameters (Figure 12)
546 were defined as the most important parameters.

547 The low influence of the *setpoint* in the sensitivity analysis results should be taken with caution.
548 Despite a mean district setpoint relatively well-known at this aggregated scale ($\pm 0.25^\circ\text{C}$), other
549 thermostat-related parameters show an influence on flexibility (e.g. *padj_{SP}*, *presence* and
550 *setback*). Moreover, some combined effects can be observed: a low set point will, for example,
551 change the effect of the ΔT due to a limit in the clothing insulation. Therefore, it is important to
552 remember that the *setpoint* controls the heating consumption and therefore plays an important
553 role in assessing the potential for flexibility.

554

555 5.1.2 Uncertainty estimation based on regression analysis

556 For each of these 7 parameters and the 2 random parameters, the coefficient of determination
557 (R^2), the mean value (mean) and the range of variation (Δ) of the shifted power are presented
558 in Figure 15 (180-minute DR event) and in Figure 16 (30-minute DR event) for the bounds
559 defined in Table 1. In both cases, relatively high values of R^2 parameter are observed for ΔT ,
560 *Qventil*, *cop*, *massThickness*, *padj_{SP}* and *padj_{clothing}*, demonstrating a correlation between the
561 variation of these parameters and the shifted power.

562 The results confirm the Morris analysis performed previously. We observe that the potential of
563 flexibility is greater in the case of short-term modulation (+ 90 W approximately). For both
564 tests, the set point decrease is also the main source of uncertainty in the district flexibility ($\Delta =$
565 100 W for the 180 min DR event, 74 W for the 30 min DR event).

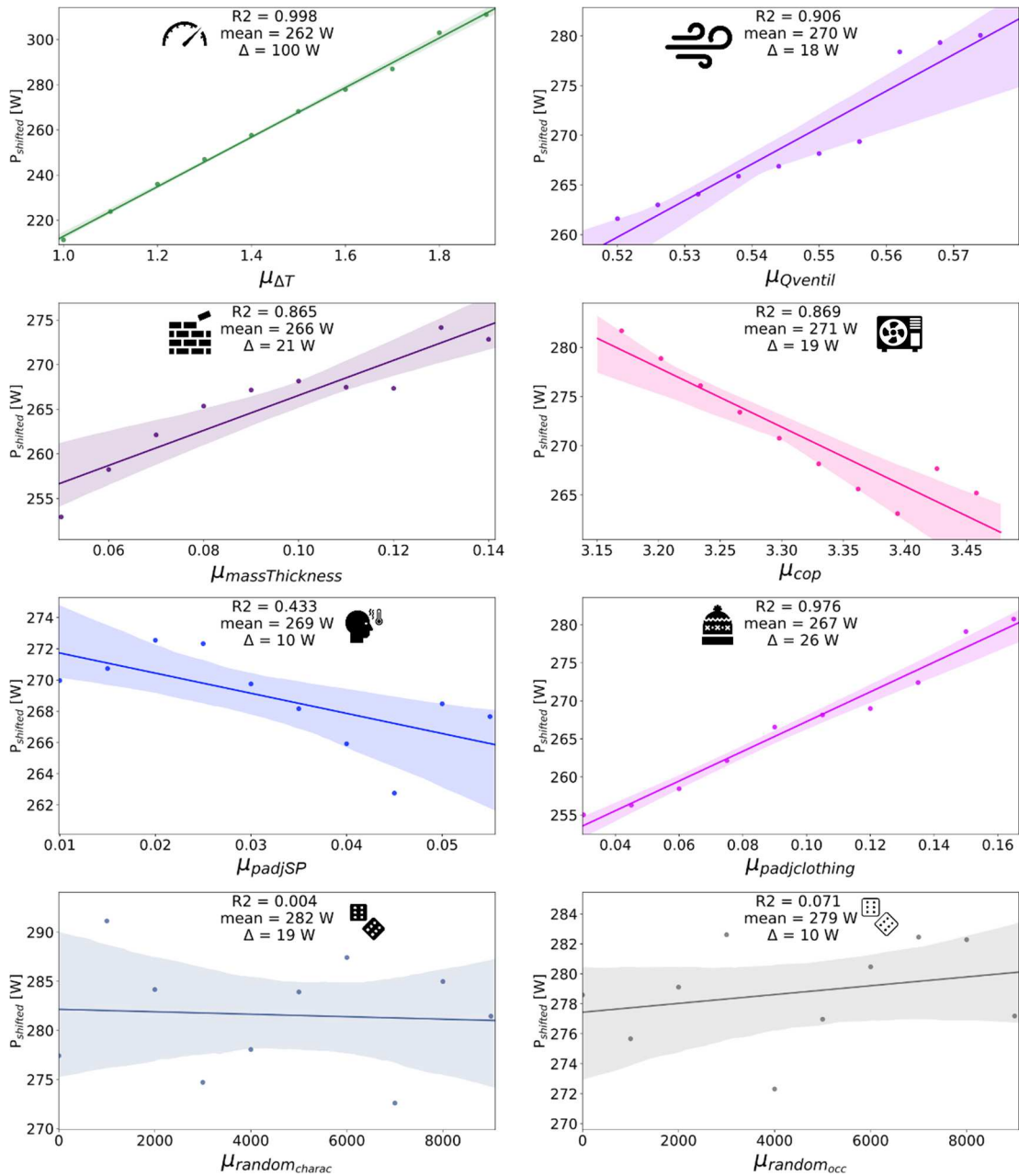
566 Parameters related to the type of occupant (*padj_{clothing}*, *padj_{SP}*, *random_{charac}* and *random_{occ}*) and
567 to the system efficiency (*cop*) are found to play a role but to a lesser extent (10-30 W). The
568 efficiency of the system plays a similar role (approximately 20 W of uncertainty) than occupant-
569 related parameters. Finally, the *massThickness* and the *Qventil*, considered as building and
570 envelope related parameter represents about 20 W of uncertainty.

571 By comparing the results for the two durations of DR events, the interaction of occupants with
572 the thermostat is discussed. For a 30-min DR event, we observe that an increase of *padj_{SP}*
573 increases the flexibility potential. This result may look unexpected, because this parameter
574 seems to be related to the possibility of rejecting flexibility, so increasing *padj_{SP}* should reduce
575 the flexibility potential. However, with the increase of *padj_{SP}*, the set temperature of residential
576 area will also increase, especially during cold days. In fact, in cold and uncomfortable
577 conditions, inhabitants are more likely to raise the set temperature. Therefore, when *padj_{SP}*
578 increases, the heating power consumption in the area will also increase. This trend is easily
579 observable in Figure 17b, where a set point difference of up to 1°C is observed between the
580 minimum and maximum values of *padj_{SP}*. This set point gap due to cold discomfort is therefore
581 maximum for the simulated period (January, coldest month of the year). Simulations made over
582 warmer periods have shown less important set point deviations.

583 Finally, due to the short duration of the event, the temperature of residential areas usually does
584 not reach its low set value, so the resident rejection is rarely observed. Therefore, in the case of
585 demand-response event of 30 min, the increase of *padj_{SP}* implies the increase of flexibility
586 potential. In the case of 180 minutes, the lower set point is more likely to be reached,
587 consequently the potential for flexibility was found to decrease with the increase of *padj_{SP}*.

588

589

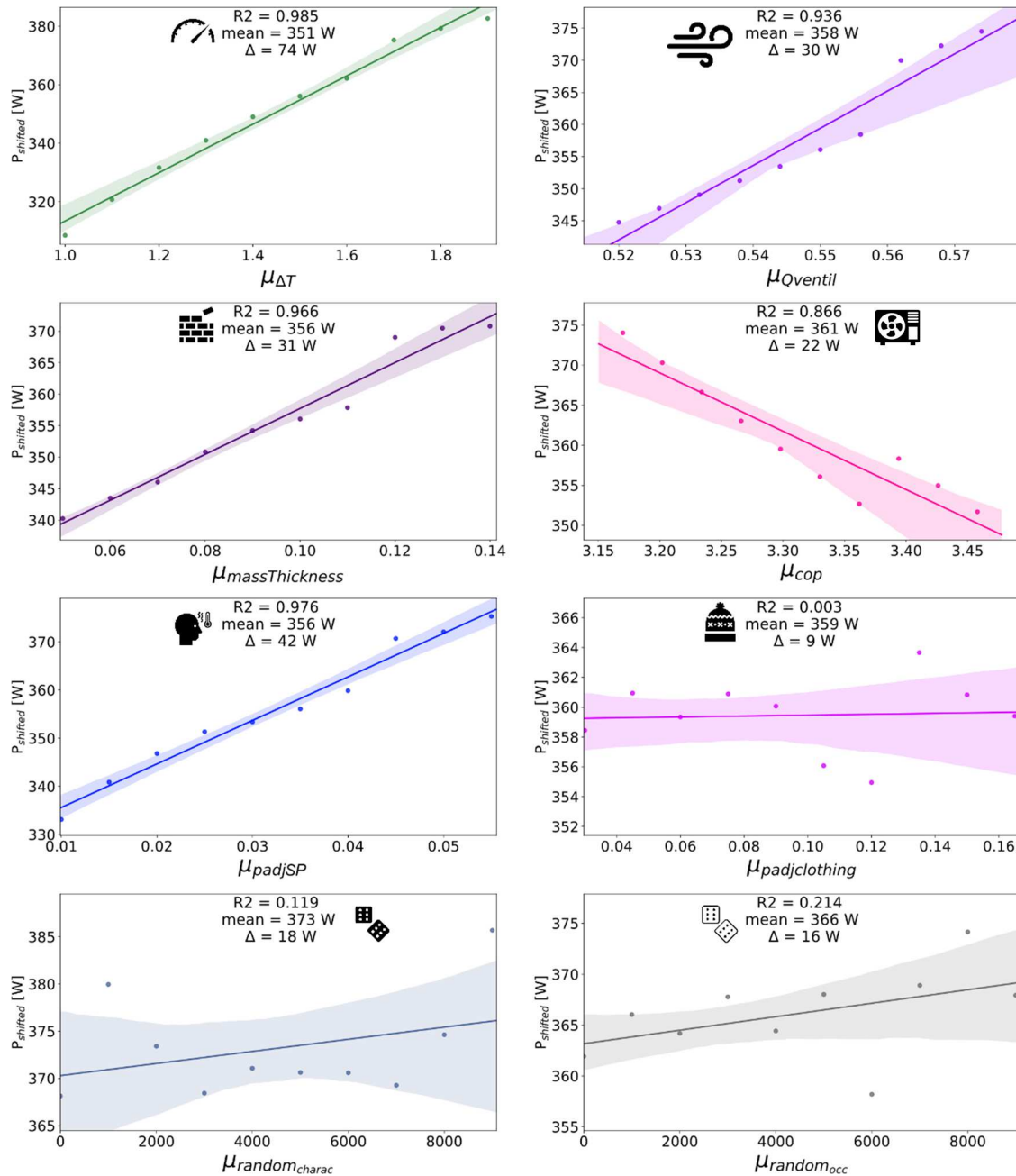


590

591

592

Figure 15 : Regression analysis for the most influential parameters on flexibility potential during the month of January (durationEvent = 180 minutes).



593

594

595

Figure 16 : Regression analysis for the most influential parameters on flexibility potential during the month of January (durationEvent = 30 minutes).

596

597

598

599

600

601

602

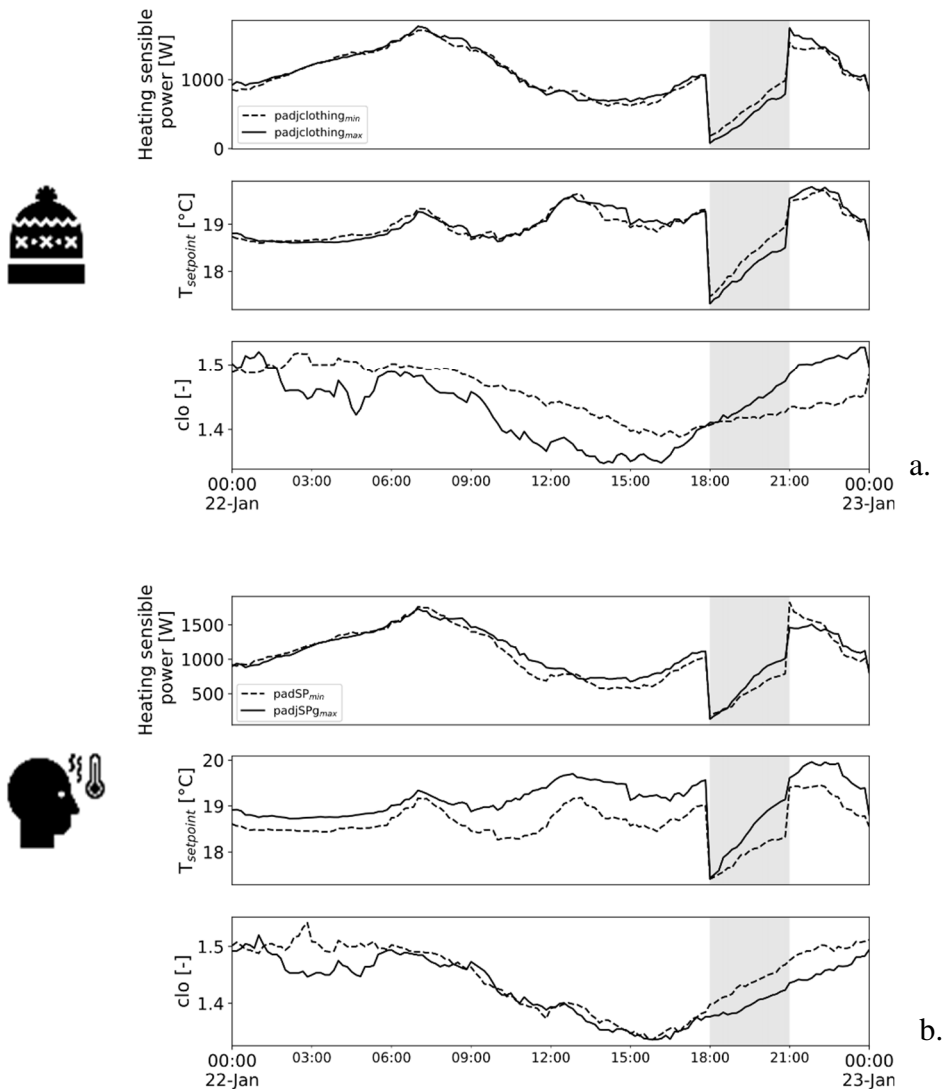
603

604

Figure 17 highlights the effect of the adjustment of the clothing insulation and the set point by the occupants on the flexibility potential. Figure 17a shows the variation of the district average heating need, set point and clothes of the neighborhood residents for a single day. The results are presented for the two extreme cases of $padjclothing_{min}$ and $padjclothing_{max}$ adjustments. As expected, the heating consumption is higher when occupants adjust less their clothing to reach their thermal comfort. Indeed, it is found that the set point is higher when the inhabitants adjust less their clothing. Finally, the last graph of Figure 17a enables to observe the dynamics of the adjustment of the clothing over the day, which are mainly due to variations of their activity-related metabolic rate.

605 Figure 17b presents the same time series but observing this time the effect of the thermostat
 606 adjustment parameter. As before, the two extreme cases of thermostat adjustment probabilities
 607 are observed: $padjSP_{min}$ and $padjSP_{max}$. We observe the effect of the thermostat adjustment by
 608 the occupants. During flexibility event, the set point is increased over time in the $padjSP_{max}$
 609 case, which reflects the occurrence of flexibility rejection.

610 Concerning the dynamics of the model outside the DR events, we observe an increase in the set
 611 point and heating consumption in the morning, as well as at lunchtime. This is mainly due to
 612 the activity of the occupants and their occupancy-related thermostat schedule. Indeed, when
 613 waking up, the occupants tend to adjust the set point temperature, as well as at lunchtime when
 614 they return home. These trends are observed in Figure 17a and Figure 17b. Concerning the
 615 evolution of the clothing coverage, we chose to represent the clothing level only for the active
 616 occupants. A decrease in clothing level during the day is observed, due to an increase in both
 617 the metabolic rate and the operative temperature.



618
 619 Figure 17 : time series of heating sensible power, set point and clothing level for the 180-min case
 620 study ('- -' : minimum value, '—': maximum value)

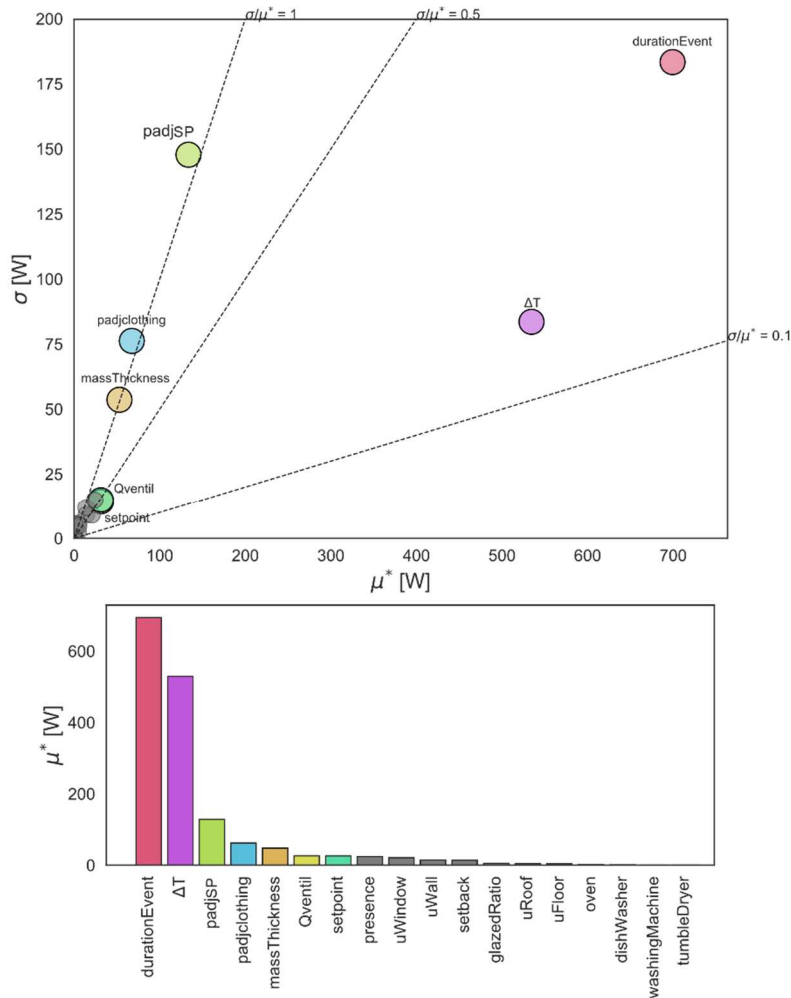
621 5.2 Old/new district comparison

622 The objective of this last study is to evaluate the importance of the building typology on the
 623 flexibility. We downgraded the building envelope properties according to the energy audit
 624 database (see Annex) giving the median values and standard deviations of U_{wall} , $U_{windows}$, U_{floor}
 625 and U_{roof} for buildings constructed during the period 1982-1989 [30]. These average values
 626 were set to 0.6, 2.98, 0.4 and 0.33 W/(m²K) respectively. It can be noticed that the standard
 627 deviations are larger than for the new district characteristics (Table 2). It should be highlighted
 628 that normal distributions might not be the best representation for partly-renovated building
 629 fabrics (log-normal distribution could be better suited [59]). However, it was decided to use
 630 normal distribution for the sake of repeatability. The heating systems are electric convectors
 631 with a thermal efficiency equal to 1, which is representative of French heating systems typical
 632 of the 1980s. With respect to the old fabric building characteristics, the average ventilation rate
 633 was increased by a factor of 1.6 to account for the higher infiltration rate and the lower
 634 ventilation efficiency.

635 Table 2 : Updated envelope and ventilation properties for the “old” district characteristics

	Name	Description	μ	σ	SA bounds [$\mu-\Delta\mu$; $\mu+\Delta\mu$]	unit
Buildings	U _{wall}	Heat loss coefficient of the walls	0.6	0.15	[0.57, 0.63]	W/(m ² K)
	U _{window}	Heat loss coefficient of the windows	2.98	0.80	[2.81, 3.15]	W/(m ² K)
	U _{floor}	Heat loss coefficient of the floor	0.4	0.15	[0.37, 0.43]	W/(m ² K)
	U _{roof}	Heat loss coefficient of the roof	0.33	0.1	[0.28, 0.32]	W/(m ² K)
	Q _{ventil}	Air change rate	0.8	0.15	[0.85, 0.91]	vol/h

636 The sensitivity analysis (Figure 18) carried out for the “old” district demonstrates an increase
 637 in the flexibility potential compared to the more recent district. Indeed, the average power
 638 shifted during January reaches 1292 W, against 290 W found previously. From a general point
 639 of view, we observe that the order of the influencing parameter remains the same. Logically,
 640 the *cop* parameter disappears for the district with electric convector and the average day set
 641 point becomes the 7-th most influential parameter. The overall increase in the μ^* parameter can
 642 be explained by the decrease in the thermal properties of the buildings. Indeed, the greater the
 643 space heating requirements, the greater the potential for flexibility.



644

645 Figure 18 : Sensitivity analysis, σ - μ^* plot and μ^* distribution for the electric power of the district
 646 during the month of January – old fabric district case study – $P_{\text{shifted avg}} = 1292 \text{ W}$

647 **5.3 Discussions**

648 Figure 19 summarizes the results of the uncertainty analysis. For each parameter, the
 649 uncertainty is calculated as the range of variation (Δ) divided by the mean value of P_{shifted} . For
 650 both types of districts, we notice that occupants have a larger influence than the building
 651 properties given a district typology. Understanding the way occupants control space heating is
 652 thus of main importance to correctly estimate flexibility. This fact indicates the need for further
 653 research in occupant behavior. Moreover, it can be observed the relatively higher uncertainty
 654 for the old district, due to the larger influence on thermal comfort. This is highlighted by the
 655 fact that the set point decrease during the DR event is important for both short and long DR
 656 events. On the contrary, short DR events in the new district decrease the influence of occupants'
 657 settings.

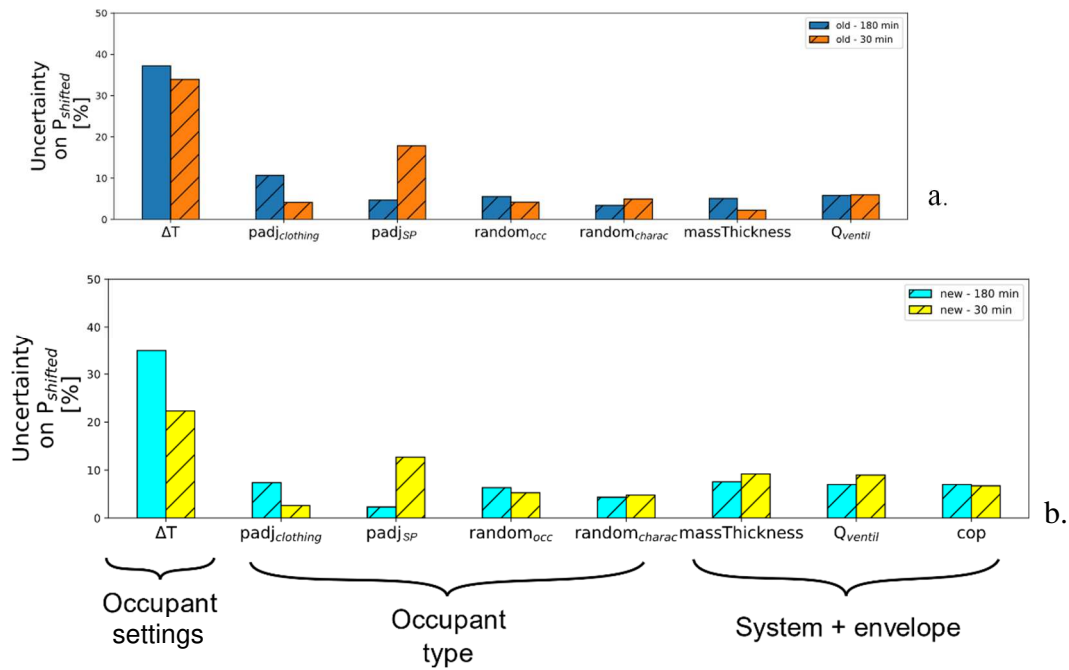


Figure 19 : Relative uncertainty on $P_{shifted}$ for the two district typologies and the two DR event durations.

658

659

660

661 Despite the broad scope of the study, some limitations should be highlighted. First of all, a
 662 district with a different compacity or with more variety of envelopes and systems might alter
 663 the conclusions. The relatively good knowledge of input data (from national databases), the
 664 homogeneity of systems and the large size of the district favored a strong decrease of some
 665 uncertainties. The evaluation of flexibility would be more challenging if some district properties
 666 are ill-known (such as construction year or type of heating system). However, this barrier should
 667 be overcome with the widespread publication of open-data on building characteristics.
 668 Furthermore, the influence of the district size has only been partly addressed in this study. An
 669 evaluation for a larger district (674 dwellings, Figure 10) was carried out and led to a slightly
 670 lower level of uncertainty.

671 Regarding the control of the heating system, a thermostat-based flexibility activation and a
 672 continuous operation of the heat pumps (*i.e.* variable-speed) were assumed. For a dense
 673 residential housing stock, this correctly represents the behavior of the heat pumps. For a single-
 674 family house equipped with a heat pump, an on/off working operation of the heat pump should
 675 be considered and would affect the availability of flexibility [51]. Changing the time of
 676 activation would also influence the flexibility.

677 Finally, only one type of occupant model was tested. Further investigation should be performed
 678 and further data should be collected to challenge the influence of occupants.

679

680

681 **6 Conclusions**

682 We have investigated the flexibility potential of a district by estimating its energy consumption
683 from a mono-zone UBEM. Flexibility or DR event were defined as a reduction in the set point
684 from 6 pm, which is classically an overloaded period of the electrical network in winter in
685 France. The occupants, building characteristics and flexibility signal were set in the model
686 according to datasets representing a current French case study. The acceptance of flexibility
687 was modeled by a thermal comfort-based model of occupant thermostat adjustments. Finally,
688 the flexibility potential was defined as the mean shifted power during DR event, and its
689 calculation has been performed for a district of 337 dwellings.

690 The positive effect of electrical load aggregation was highlighted in the prediction of the
691 electrical load at district level, with a decrease of the uncertainty for groups of more than 50
692 dwellings. Once the UBEM model was built, a sensitivity analysis and a linear regression
693 analysis were performed to identify the most influential parameters on the results and to better
694 understand the sources of uncertainty on the flexibility potential.

695 For this winter case study, the space heating represents the greatest potential for flexibility, so
696 we did not consider the flexibility potential on other appliances or systems. The results show
697 the influence of modulation time and set point decrease during demand response event,
698 occupant types and activities. The order of magnitude of the flexibility potential is about 290 W
699 per household for the new district and about 1290 W for the old district. Several key points
700 should be emphasized:

- 701 ▪ This study shows the great importance of the duration of the flexibility signal on the
702 results. It appears to be one of the most influential parameters, so it must be carefully
703 selected by the aggregator to optimize the flexibility portfolio.
- 704 ▪ Considering DR event duration, it appears that a long-DR events lead to a decrease in
705 the shiftable power. A tradeoff between the power decrease and the duration of
706 activation should thus be defined to optimally activate flexibility.
- 707 ▪ Occupants appear to play a key role in flexibility. The dynamic modelling of occupant
708 behavior was carried out and allows the quantification of the occupant rejection
709 phenomenon. The behavior of occupants must be carefully taken into account when
710 estimating the flexibility potential.
- 711 ▪ Finally, the characteristics of the buildings did not show a too large uncertainty in the
712 resulting flexibility at district level. Indeed, the aggregation effect was sufficient enough
713 to dampen the diversity observed in the building databases. This conclusion is valid only
714 if the construction period and the heating system are roughly known.

715 This work paves the way of the flexibility characterization at district level by quantifying the
716 source of uncertainties using a UBEM model. In future work, a focus on the most influencing
717 parameter can be done, while considering fewer other parameters with less influence, which
718 can improve the efficiency of the characterization of flexibility. Moreover, the strong influence
719 of climate and flexibility signal underlines the future need for “smart” controllers in buildings.

720 **7 Acknowledgements**

721 This research was funded by the French National Research Agency, CLEF project (ANR-17-
722 CE22-0005-01).

723

724 **Annex: Summary of the used datasets**

725

Category	Name	Type	Geographical area	Year of data collection	Size	Ref.
National grid	RTE (residual load)	Database	France	2017	-	[60]
Geometry	BDTOPO (land register)	Database	France	2020	-	[61]
Buildings	DPE (energy audit of existing buildings)	Database	Department (Charente-Maritime, 17)	2013-2020	71 000 households, 1831 of similar type	[62]
	RT 2012 (new building regulation)	Database	Metropolitan France	2012-2020	136 811 households	[55]
	OQAI survey (ventilation rates)	Survey	Metropolitan France	2003–2005	567 households	[33]
Occupants	Population census (household composition et taux d'équipement)	Survey	Metropolitan France	2010-2015	28 million households	[64]
	Time Use Survey (activities)	Survey	Metropolitan France	2009-2010	13 950 individuals from 12 000 households	[65]
	EcoBee (smart thermostats)	Appliance Monitoring	Canada	2015-2020	9 000 households	[43]
	PHEBUS survey (heating habits and appliances ownership)	Survey	Metropolitan France	2013	5 345 households	[66]
	PEDOBUR and EQL'ORE projects (usage based on ToU)	Survey	La Rochelle, France	2019	99 households	x
	LINEAR project (shifting probabilities)	Appliance Monitoring	Flanders region, Belgium	2009-2014	186 households	[67]
Appliances	EU energy labelling of appliances (energy efficiency)	Regulation	Europe		-	[68]
	TOPTEN-Ademe (energy class and size)	Market data	France	2004-2014	90% of market	[69]
	REMODECE project (energy class and size)	Appliance Monitoring	Auvergne-Rhône-Alpes region, France	2008	103 households	[70]
	FROIDLAVAGE monitoring campaign (usage)	Appliance Monitoring	Metropolitan France	2015-2016	107 households	[71]
	ADEME survey campaign (usage)	Survey	Metropolitan France	2015	1 001 households	[72]

726

727 **References**

- 728 [1] P.D. Lund, J. Lindgren, J. Mikkola, J. Salpakari, Review of energy system flexibility measures
729 to enable high levels of variable renewable electricity, *Renewable and Sustainable Energy*
730 *Reviews*. 45 (2015) 785–807. <https://doi.org/10.1016/j.rser.2015.01.057>.
- 731 [2] World Business Council for Sustainable Development, *Transforming the Market*, 2009.
732 [https://www.wbcsd.org/Programs/Cities-and-Mobility/Resources/Transforming-the-](https://www.wbcsd.org/Programs/Cities-and-Mobility/Resources/Transforming-the-Market-Energy-Efficiency-in-Buildings)
733 [Market-Energy-Efficiency-in-Buildings](https://www.wbcsd.org/Programs/Cities-and-Mobility/Resources/Transforming-the-Market-Energy-Efficiency-in-Buildings).
- 734 [3] IEA, IEA report, Chap. 6 Buildings sector energy consumption, (2016).
735 <https://www.eia.gov/outlooks/ieo/pdf/buildings.pdf> (accessed September 25, 2020).
- 736 [4] K.M. Luc, R. Li, L. Xu, T.R. Nielsen, J.L.M. Hensen, Energy flexibility potential of a small
737 district connected to a district heating system, *Energy and Buildings*. 225 (2020) 110074.
738 <https://doi.org/10.1016/j.enbuild.2020.110074>.
- 739 [5] S.Ø. Jensen, A. Marszal-Pomianowska, R. Lollini, W. Pasut, A. Knotzer, P. Engelmann, A.
740 Stafford, G. Reynders, IEA EBC Annex 67 Energy Flexible Buildings, *Energy and Buildings*.
741 155 (2017) 25–34. <https://doi.org/10.1016/j.enbuild.2017.08.044>.
- 742 [6] H. Johra, P. Heiselberg, J. Le Dréau, Influence of envelope, structural thermal mass and
743 indoor content on the building heating energy flexibility, *Energy and Buildings*. 183 (2019)
744 325–339. <https://doi.org/10.1016/j.enbuild.2018.11.012>.
- 745 [7] M. Hu, F. Xiao, Quantifying uncertainty in the aggregate energy flexibility of high-rise
746 residential building clusters considering stochastic occupancy and occupant behavior,
747 *Energy*. 194 (2020) 116838. <https://doi.org/10.1016/j.energy.2019.116838>.
- 748 [8] J. Dickert, P. Schegner, Residential Load Models for Network Planning Purposes, (n.d.) 7.
- 749 [9] I.D. Jaeger, G. Reynders, D. Saelens, T. Park, Quantifying Uncertainty Propagation For The
750 District Energy Demand Using Realistic Variations On Input Data, in: 2019.
751 <https://doi.org/10.26868/25222708.2019.210923>.
- 752 [10] J. Sala, R. Li, M.H. Christensen, Clustering and classification of energy meter data: A
753 comparison analysis of data from individual homes and the aggregated data from
754 multiple homes, *Build. Simul.* 14 (2021) 103–117. [https://doi.org/10.1007/s12273-019-](https://doi.org/10.1007/s12273-019-0587-4)
755 [0587-4](https://doi.org/10.1007/s12273-019-0587-4).
- 756 [11] Y.Q. Ang, Z.M. Berzolla, C.F. Reinhart, From concept to application: A review of use cases
757 in urban building energy modeling, *Applied Energy*. 279 (2020) 115738.
758 <https://doi.org/10.1016/j.apenergy.2020.115738>.
- 759 [12] M. Ferrando, F. Causone, T. Hong, Y. Chen, Urban building energy modeling (UBEM) tools:
760 A state-of-the-art review of bottom-up physics-based approaches, *Sustainable Cities and*
761 *Society*. 62 (2020) 102408. <https://doi.org/10.1016/j.scs.2020.102408>.
- 762 [13] F. Johari, G. Peronato, P. Sadeghian, X. Zhao, J. Widén, Urban building energy modeling:
763 State of the art and future prospects, *Renewable and Sustainable Energy Reviews*. 128
764 (2020) 109902. <https://doi.org/10.1016/j.rser.2020.109902>.
- 765 [14] C.F. Reinhart, C. Cerezo Davila, Urban building energy modeling – A review of a nascent
766 field, *Building and Environment*. 97 (2016) 196–202.
767 <https://doi.org/10.1016/j.buildenv.2015.12.001>.
- 768 [15] I. De Jaeger, J. Lago, D. Saelens, A probabilistic building characterization method for
769 district energy simulations, *Energy and Buildings*. 230 (2021) 110566.
770 <https://doi.org/10.1016/j.enbuild.2020.110566>.

- 771 [16] D.V. Likhachev, Parametric sensitivity analysis as an essential ingredient of spectroscopic
772 ellipsometry data modeling: An application of the Morris screening method, *Journal of*
773 *Applied Physics*. 126 (2019) 184901. <https://doi.org/10.1063/1.5126074>.
- 774 [17] J. Vivian, U. Chiodarelli, G. Emmi, A. Zarrella, A sensitivity analysis on the heating and
775 cooling energy flexibility of residential buildings, *Sustainable Cities and Society*. 52 (2020)
776 101815. <https://doi.org/10.1016/j.scs.2019.101815>.
- 777 [18] Z. Ma, A. Knotzer, J.D. Billanes, B.N. Jørgensen, A literature review of energy flexibility in
778 district heating with a survey of the stakeholders' participation, *Renewable and*
779 *Sustainable Energy Reviews*. 123 (2020) 109750.
780 <https://doi.org/10.1016/j.rser.2020.109750>.
- 781 [19] F. Scarpa, L.A. Tagliafico, V. Bianco, Financial and energy performance analysis of efficiency
782 measures in residential buildings. A probabilistic approach, *Energy*. 236 (2021) 121491.
783 <https://doi.org/10.1016/j.energy.2021.121491>.
- 784 [20] V. Masson, J. Hidalgo, A. Amossé, F. Belaid, E. Bocher, M. Bonhomme, A. Bourgeois, G.
785 Bretagne, S. Caillerez, E. Cordeau, C. Demazeux, S. Faraut, C. Gallato, S. Haouès-Jouve, M.-
786 L. Lambert, A. Lemonsu, R. Lestringant, J.-P. Levy, N. Long, C.X. Lopez, M. Pellegrino, G.
787 Petit, C. Pignon-Mussaud, C. Plumejeaud-Perreau, V. Ruff, R. Schoetter, N. Tornay, D.D.
788 Vye, *Urban Climate, Human behavior & Energy consumption: from LCZ mapping to*
789 *simulation and urban planning (the MapUCE project)*, in: 9th International Conference on
790 *Urban Climate*, CNRM - Météo France, Toulouse, France, 2015. [https://hal.archives-](https://hal.archives-ouvertes.fr/hal-01252761)
791 [ouvertes.fr/hal-01252761](https://hal.archives-ouvertes.fr/hal-01252761) (accessed September 28, 2020).
- 792 [21] M. Vellei, S. Martinez, J. Le Dréau, Agent-based stochastic model of thermostat
793 adjustments: A demand response application, *Energy and Buildings*. 238 (2021) 110846.
794 <https://doi.org/10.1016/j.enbuild.2021.110846>.
- 795 [22] Smart Thermostats & Smart Home Devices | ecobee, (n.d.). [https://www.ecobee.com/en-](https://www.ecobee.com/en-us/)
796 [us/](https://www.ecobee.com/en-us/) (accessed March 17, 2021).
- 797 [23] P. Riederer, V. Partenay, N. Perez, C. Nocito, R. Trigance, T. Guiot, Development of a
798 simulation platform for the evaluation of district energy system performances, (2015).
799 <https://doi.org/10.13140/RG.2.1.4668.8401/1>.
- 800 [24] N. Perez, P. Riederer, C. Inard, V. Partenay, Thermal building modelling adapted to district
801 energy simulation, (2015). <https://doi.org/10.13140/RG.2.1.3714.2163/1>.
- 802 [25] E. Garreau, Y. Abdelouadoud, E. Herrera, W. Keilholz, G.-E. Kyriakodis, V. Partenay, P.
803 Riederer, District MOdeller and SIMulator (DIMOSIM) – A dynamic simulation platform
804 based on a bottom-up approach for district and territory energetic assessment, *Energy*
805 *and Buildings*. 251 (2021) 111354. <https://doi.org/10.1016/j.enbuild.2021.111354>.
- 806 [26] L. Frayssinet, Adapting buildings heating and cooling power need models at the district
807 scale, (n.d.) 253.
- 808 [27] J. Sokol, C. Cerezo Davila, C.F. Reinhart, Validation of a Bayesian-based method for
809 defining residential archetypes in urban building energy models, *Energy and Buildings*.
810 134 (2017) 11–24. <https://doi.org/10.1016/j.enbuild.2016.10.050>.
- 811 [28] seaborn.distplot — seaborn 0.11.2 documentation, (n.d.).
812 <https://seaborn.pydata.org/generated/seaborn.distplot.html> (accessed September 6,
813 2021).
- 814 [29] M. Shin, J.S. Haberl, Thermal zoning for building HVAC design and energy simulation: A
815 literature review, *Energy and Buildings*. 203 (2019) 109429.
816 <https://doi.org/10.1016/j.enbuild.2019.109429>.

- 817 [30] Observatoire des performances énergétiques (OPE) - data.gouv.fr, (n.d.).
818 <https://www.data.gouv.fr/fr/datasets/observatoire-des-performances-energetiques/>
819 (accessed September 23, 2020).
- 820 [31] Diagnostics de performance énergétique pour les logements par habitation - data.gouv.fr,
821 (n.d.). [/fr/datasets/diagnostics-de-performance-energetique-pour-les-logements-par-](https://www.data.gouv.fr/fr/datasets/diagnostics-de-performance-energetique-pour-les-logements-par-habitation/)
822 [habitation/](https://www.data.gouv.fr/fr/datasets/diagnostics-de-performance-energetique-pour-les-logements-par-habitation/) (accessed January 15, 2021).
- 823 [32] O. Ruhnau, L. Hirth, A. Praktijnjo, Time series of heat demand and heat pump efficiency
824 for energy system modeling, *Sci Data*. 6 (2019) 189. [https://doi.org/10.1038/s41597-019-](https://doi.org/10.1038/s41597-019-0199-y)
825 [0199-y](https://doi.org/10.1038/s41597-019-0199-y).
- 826 [33] S. Langer, O. Ramalho, M. Derbez, J. Ribéron, S. Kirchner, C. Mandin, Indoor environmental
827 quality in French dwellings and building characteristics, *Atmospheric Environment*. 128
828 (2016) 82–91. <https://doi.org/10.1016/j.atmosenv.2015.12.060>.
- 829 [34] M. Vellei, J. Le Dréau, S.Y. Abdelouadoud, Predicting the demand flexibility of wet
830 appliances at national level: The case of France, *Energy and Buildings*. 214 (2020) 109900.
831 <https://doi.org/10.1016/j.enbuild.2020.109900>.
- 832 [35] M. Vellei, J.L. Dréau, On the prediction of dynamic thermal comfort under uniform
833 environments, in: 2020: p. 424. [https://hal-univ-rochelle.archives-ouvertes.fr/hal-](https://hal-univ-rochelle.archives-ouvertes.fr/hal-02556047)
834 [02556047](https://hal-univ-rochelle.archives-ouvertes.fr/hal-02556047) (accessed March 17, 2021).
- 835 [36] M. Vellei, S. Martinez, J. Le Dréau, Agent-based stochastic model of thermostat
836 adjustments: a demand response application, *Energy and Buildings*. (2021) 110846.
837 <https://doi.org/10.1016/j.enbuild.2021.110846>.
- 838 [37] Statistical presentation – Statistics on income and living conditions 2010 | Insee, (n.d.).
839 <https://www.insee.fr/en/metadonnees/source/operation/s1074/presentation> (accessed
840 January 15, 2021).
- 841 [38] Statistical presentation – Time use survey 2009-2010 | Insee, (n.d.).
842 <https://www.insee.fr/en/metadonnees/source/operation/s1362/presentation> (accessed
843 November 17, 2020).
- 844 [39] B.F. Balvedi, E. Ghisi, R. Lamberts, A review of occupant behaviour in residential buildings,
845 *Energy and Buildings*. 174 (2018) 495–505. <https://doi.org/10.1016/j.enbuild.2018.06.049>.
- 846 [40] ANSI/ASHRAE Addendum g to ANSI/ASHRAE Standard 55-2010, (n.d.) 8.
- 847 [41] Enquête Performance de l’Habitat, Équipements, Besoins et Usages de l’énergie (Phébus)
848 | Données et études statistiques, (n.d.). [https://www.statistiques.developpement-](https://www.statistiques.developpement-durable.gouv.fr/enquete-performance-de-lhabitat-equipements-besoins-et-usages-de-lenergie-phebus)
849 [durable.gouv.fr/enquete-performance-de-lhabitat-equipements-besoins-et-usages-de-](https://www.statistiques.developpement-durable.gouv.fr/enquete-performance-de-lhabitat-equipements-besoins-et-usages-de-lenergie-phebus)
850 [lenergie-phebus](https://www.statistiques.developpement-durable.gouv.fr/enquete-performance-de-lhabitat-equipements-besoins-et-usages-de-lenergie-phebus) (accessed January 15, 2021).
- 851 [42] Ademe, *Projet PECOIC - Prise en compte du comportement des occupants et incertitudes*
852 *associées en phase conception de bâtiments*, 2019.
- 853 [43] Donate your Data Smart Wi-Fi Thermostats by ecobee, (n.d.).
854 <https://www.ecobee.com/donate-your-data/> (accessed November 17, 2020).
- 855 [44] M. Humphreys, F. Nicol, S. Roaf, *Adaptive Thermal Comfort: Foundations and Analysis*,
856 Taylor & Francis Group, London, 2015.
- 857 [45] A.S. Rao, M.P. Georgeff, BDI Agents: From Theory to Practice, in: *ICMAS95: 1st*
858 *INTERNATIONAL CONFERENCE ON MULTI-AGENT SYSTEMS*, San Francisco (USA), 1995.
859 <https://doi.org/10.1.1.37.7970>.
- 860 [46] F. Tartarini, S. Schiavon, T. Cheung, T. Hoyt, CBE Thermal Comfort Tool: Online tool for
861 thermal comfort calculations and visualizations, *SoftwareX*. 12 (2020) 100563.
862 <https://doi.org/10.1016/j.softx.2020.100563>.

- 863 [47] BESTEST-EX: Building Energy Simulation Test for Existing Homes, (n.d.).
864 <https://www.nrel.gov/buildings/bestest-ex.html> (accessed February 18, 2021).
- 865 [48] D. Saelens, I. De Jaeger, F. Bünnig, M. Mans, A. Maccarini, E. Garreau, Ø. Rønneseth, I.
866 Sartori, A. Vandermeulen, B. van der Heijde, L. Helsen, Towards a DESTEST: a District
867 Energy Simulation Test Developed in IBPSA Project 1, 2019.
868 <https://doi.org/10.26868/25222708.2019.210806>.
- 869 [49] É. Vorger, Étude de l'influence du comportement des habitants sur la performance
870 énergétique du bâtiment, phdthesis, Ecole Nationale Supérieure des Mines de Paris, 2014.
871 <https://pastel.archives-ouvertes.fr/tel-01144461> (accessed November 19, 2020).
- 872 [50] Å.L. Sørensen, I. Sartori, K.B. Lindberg, I. Andresen, Electricity analysis for energy
873 management in neighbourhoods: Case study of a large housing cooperative in Norway,
874 1343. (2019). <https://ntnuopen.ntnu.no/ntnu-xmlui/handle/11250/2629829> (accessed
875 November 19, 2020).
- 876 [51] D. Fischer, T. Wolf, J. Wapler, R. Hollinger, H. Madani, Model-based flexibility assessment
877 of a residential heat pump pool, *Energy*. 118 (2017) 853–864.
878 <https://doi.org/10.1016/j.energy.2016.10.111>.
- 879 [52] European smart grids task force, Final report: demand side flexibility, perceived barriers
880 and proposed recommendations, 2019.
881 https://ec.europa.eu/energy/sites/ener/files/documents/eg3_final_report_demand_side_flexibility_2019.04.15.pdf (accessed February 10, 2021).
- 882 [53] A. Wang, R. Li, S. You, Development of a data driven approach to explore the energy
883 flexibility potential of building clusters, *Applied Energy*. 232 (2018) 89–100.
884 <https://doi.org/10.1016/j.apenergy.2018.09.187>.
- 885 [54] M.D. Morris, Factorial Sampling Plans for Preliminary Computational Experiments,
886 *Technometrics*. 33 (1991) 161–174. <https://doi.org/10.2307/1269043>.
- 887 [55] E. Borgonovo, E. Plischke, Sensitivity analysis: A review of recent advances, *European
888 Journal of Operational Research*. 248 (2016) 869–887.
889 <https://doi.org/10.1016/j.ejor.2015.06.032>.
- 890 [56] B. Iooss, P. Lemaître, A Review on Global Sensitivity Analysis Methods, in: G. Dellino, C.
891 Meloni (Eds.), *Uncertainty Management in Simulation-Optimization of Complex Systems:
892 Algorithms and Applications*, Springer US, Boston, MA, 2015: pp. 101–122.
893 https://doi.org/10.1007/978-1-4899-7547-8_5.
- 894 [57] J.D. Herman, J.B. Kollat, P.M. Reed, T. Wagener, Technical note: Method of Morris
895 effectively reduces the computational demands of global sensitivity analysis for
896 distributed watershed models, *Hydrol. Earth Syst. Sci. Discuss.* 10 (2013) 4275–4299.
897 <https://doi.org/10.5194/hessd-10-4275-2013>.
- 898 [58] W. Tian, Y. Heo, P. de Wilde, Z. Li, D. Yan, C.S. Park, X. Feng, G. Augenbroe, A review of
899 uncertainty analysis in building energy assessment, *Renewable and Sustainable Energy
900 Reviews*. 93 (2018) 285–301. <https://doi.org/10.1016/j.rser.2018.05.029>.
- 901 [59] G. Petrou, A. Mavrogianni, P. Symonds, M. Davies, Beyond Normal: Guidelines on How to
902 Identify Suitable Model Input Distributions for Building Performance Analysis, (n.d.) 8.
- 903 [60] Schedule of Tempo-type supply offerings - RTE Services Portal, Portail Services RTE. (n.d.).
904 [https://www.services-rte.com/en/view-data-published-by-rte/schedule-of-Tempo-type-
905 supply-offerings.html](https://www.services-rte.com/en/view-data-published-by-rte/schedule-of-Tempo-type-supply-offerings.html) (accessed March 12, 2021).
- 906

- 907 [61] Géoservices | Accéder au téléchargement des données libres IGN, (n.d.).
908 <https://geoservices.ign.fr/documentation/diffusion/telechargement-donnees-libres.html>
909 (accessed March 12, 2021).
- 910 [62] ADEME, Diagnostics de performance énergétique pour les logements par habitation,
911 (2020). <https://data.ademe.fr/datasets/dpe-france> (accessed March 17, 2021).
- 912 [63] Observatoire des performances énergétiques (OPE) - data.gouv.fr, (n.d.).
913 [/fr/datasets/observatoire-des-performances-energetiques/](https://data.gouv.fr/datasets/observatoire-des-performances-energetiques/) (accessed March 18, 2021).
- 914 [64] INSEE, 2015 Population census, (2015).
915 <https://www.insee.fr/en/metadonnees/source/serie/s1321>.
- 916 [65] INSEE, 2009-2010 Time Use Survey, (2010).
917 <https://www.insee.fr/en/metadonnees/source/operation/s1362/presentation>.
- 918 [66] SDES, PHEBUS CLODE: Enquête Performance de l'Habitat, Equipements, Besoins et
919 USages de l'énergie - volet CLODE, 2013.
- 920 [67] R. D'hulst, W. Labeeuw, B. Beusen, S. Claessens, G. Deconinck, K. Vanthournout, Demand
921 response flexibility and flexibility potential of residential smart appliances: Experiences
922 from large pilot test in Belgium, *Applied Energy*. 155 (2015) 79–90.
923 <https://doi.org/10.1016/j.apenergy.2015.05.101>.
- 924 [68] Commission Delegated Regulation (EU) No 392/2012 of 1 March 2012 supplementing
925 Directive 2010/30/EU of the European Parliament and of the Council with regard to
926 energy labelling of household tumble driersText with EEA relevance, (n.d.) 26.
- 927 [69] Energy efficiency of White Goods in Europe: monitoring the market with sales ..., ADEME.
928 (n.d.). [https://www.ademe.fr/energy-efficiency-of-white-goods-in-europe-monitoring-](https://www.ademe.fr/energy-efficiency-of-white-goods-in-europe-monitoring-the-market-with-sales-data-0)
929 [the-market-with-sales-data-0](https://www.ademe.fr/energy-efficiency-of-white-goods-in-europe-monitoring-the-market-with-sales-data-0) (accessed March 17, 2021).
- 930 [70] A. de Almeida, P. Fonseca, B. Schlomann, N. Feilberg, C. Ferreira, Residential Monitoring
931 to Decrease Energy Use and Carbon Emissions in Europe (REMODECE), 2008.
- 932 [71] Campagne de mesures des appareils de production de froid, des appareils de lavage et
933 de la climatisation, (2016) 179.
- 934 [72] Etude Usage Lavage Domestique, ADEME. (n.d.). [https://www.ademe.fr/etude-usage-](https://www.ademe.fr/etude-usage-lavage-domestique)
935 [lavage-domestique](https://www.ademe.fr/etude-usage-lavage-domestique) (accessed March 18, 2021).
- 936
- 937